1866

# D02, A Novel, Non-Blocking Antibody Targeting IL2RA, Exhibits Significant Anti-Tumor Activity in IL2RA-Humanized Mice

Yongfei Yang, Wenjiao Zhang, Shuzhen Cao, Qingcong Lin, Yue Yan, Luheng Du, Zeliang Guan, Jing Zhang, Qingya Duan, Yacui Liu
Biocytogen Pharmaceuticals (Beijing) Co., Ltd., Beijing, China

BIOCYTOGEN

biocytogen.com | info@biocytogen.com

## ABSTRACT

T regulatory cells, or Tregs, are a subset of CD4+ T cells that negatively regulate immune responses to promote their resolution and protect against autoimmunity. Infiltration of Tregs in the tumor microenvironment (TME), and a low ratio of effector T cells to Tregs, is frequently associated with tumor progression and poor prognosis. The alpha subunit of the IL-2 cytokine receptor (IL2RA), a component of the high-affinity IL-2 receptor along with the β-subunit (IL2RB), is highly expressed on Tregs. IL-2 is a key cytokine for effector T cell survival and cytolytic responses. We aimed to discover an IL2RA-targeting antibody capable of depleting Tregs but permitting IL-2 stimulation of effector T cells in the TME.

We developed a fully human IgG1 antibody specific to IL2RA, D02, from our proprietary RenMab™ mice, which contain the entire human immunoglobulin variable domain. D02 binds both human and cynomolgus monkey IL2RA with high affinity without hindering IL2RA-IL-2 binding or inhibiting IL-2 signaling. To evaluate the safety and efficacy of D02 in vivo, we established a syngeneic mouse tumor model in IL2RA-humanized mice. We observed that D02 potently inhibited MC38 (colon adenocarcinoma) tumor growth at 10 mg/kg. Further studies will aim to characterize the effect of D02 on the ratio of effector T cells to Tregs in the TME. These data indicate that D02 is a novel, IL2RA-specific monoclonal antibody that uniquely exhibits significant anti-tumor activity *in vivo* while preserving IL-2 signaling to effector T cells.

## High affinity binding of D02 to both hIL2RA and fasIL2RA

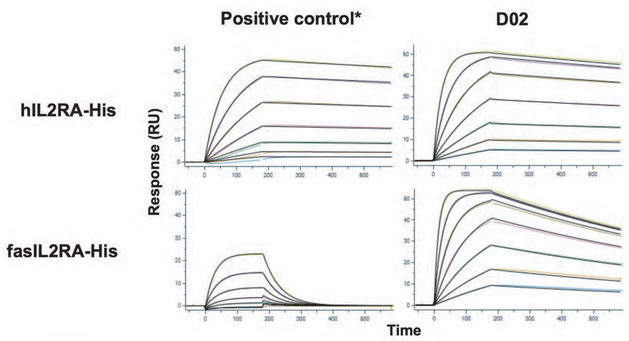


| | Analyte Solution | ka (1/Ms) | kd (1/s) | KD (M) |
|---|---|---|---|---|
| Positive control* | hIL2RA-His | 9.4E+04 | 1.7E-04 | 1.9E-09 |
| | fasIL2RA-His | 7.4E+04 | 2.0E-02 | 2.6E-07 |
| D02 | hIL2RA-His | 1.9E+05 | 2.4E-04 | 1.3E-09 |
| | fasIL2RA-His | 3.6E+05 | 9.0E-04 | 2.5E-09 |

*The positive control is 7G7B6-IgG1-SI

**Affinity kinetics of multiple antibody concentrations measured by surface plasmon resonance (SPR).**

## D02 demonstrates good binding activity

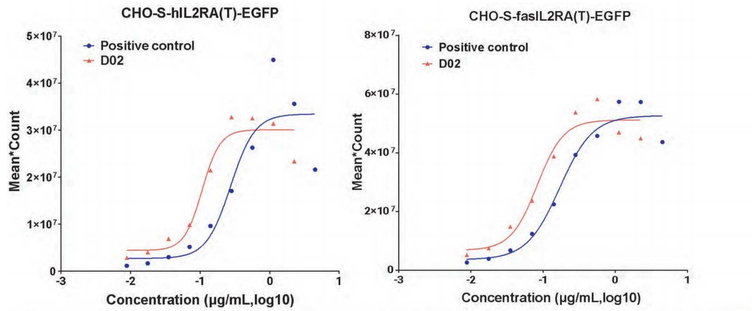


| Sample | CHO-S-hIL2RA(T)-EGFP | | CHO-S-fasIL2RA(T)-EGFP | |
|---|---|---|---|---|
| | EC50 | R square | EC50 | R square |
| Positive control | 0.08 | 0.972 | 0.06 | 0.994 |
| D02 | 0.05 | 0.971 | 0.04 | 0.990 |

**Binding activity of D02 and positive control antibody (7G7B6) to human and cynomolgus monkey IL2RA. Total positive fluorescence intensity was measured by flow cytometry.**

## D02 binds to the sushi2 epitope of the human IL-2 receptor

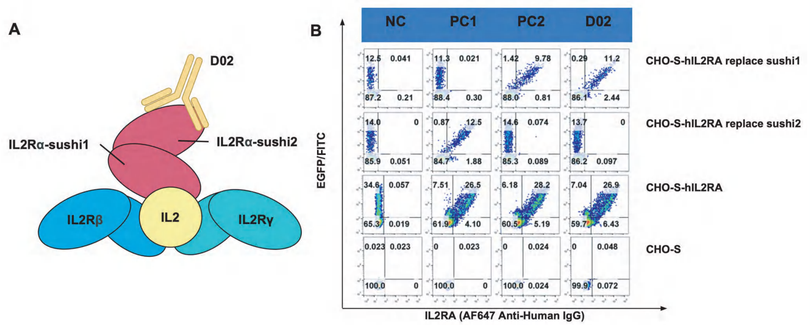


**Epitope binding results based on flow cytometry data.** (A) Diagram of the human IL-2 signaling complex. 82% of IL2RA-sushi1 is buried at the IL2/IL2RA junction, but only a small fraction of IL2RA-sushi2 is buried in the junction. (B) Antibody D02 and a non-blocking positive control antibody (PC2) did not bind IL2RA lacking hIL2RA-sushi2. PC1: Daclizumab (blocking antibody), PC2: 7G7B6-IgG1-SI (non-blocking antibody).

## D02 is a non-blocking IL2RA antibody

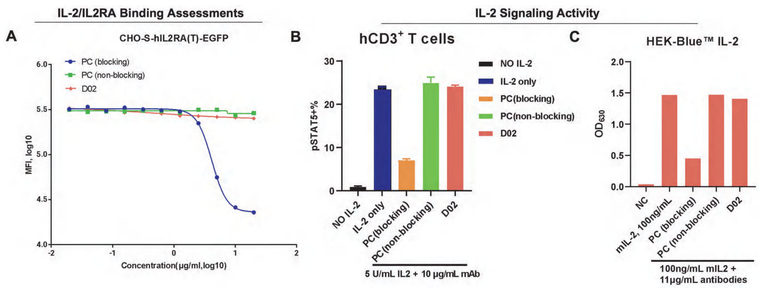


**Assessment of IL2RA signaling activity in the presence of D02.** (A) D02 did not block the binding of IL2RA ligand (human IL-2) with IL2RA; (B) D02 did not impact human IL2-induced STAT5 phosphorylation. Experiments were conducted using flow cytometry. Error bars indicate SD. (C) IL2 reporter cell blockade assay. HEK-Blue™ IL-2 reporter cells containing a STAT5-inducible SEAP (secreted embryonic alkaline phosphatase; InvivoGen) were used to quantify IL-2-mediated STAT5 activation. D02 did not block the binding of mouse IL-2 to the IL-2 reporter cells. Blocking PC: Daclizumab; Non-blocking PC2: 7G7B6-IgG1-SI.

## D02 reduces MC38 tumor volume *in vivo*

**Anti-tumor activity of D02.** MC38 tumors were implanted in humanized B-hIL2RA mice and treated with 10 mg/kg antibody, i.p., BIW×6. D02 showed a better tumor inhibitory effect compared with PBS and the positive control (7G7B6-IgG1-SI) groups. TGI: tumor growth inhibition. Error bars indicate SD.

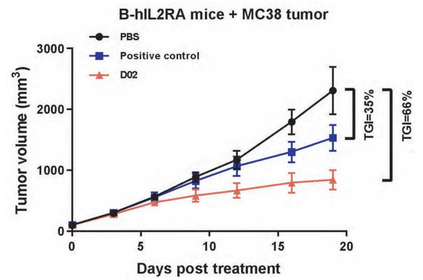


## CONCLUSIONS

- D02 is a fully human IgG1 antibody specific to IL2RA that was obtained from RenMab™ humanized immunoglobulin mice.
- D02 binds both human and cynomolgus monkey IL2RA with high affinity.
- D02 binds to the sushi2 epitope of IL2RA without obstructing the binding of IL-2 or inhibiting IL-2 signaling.
- D02 exhibits anti-tumor efficacy when administered to mice harboring MC38 tumors.

6436

# 1C3, a novel non-blocking anti-human TNFR2 antibody, promotes effector T cell responses and demonstrates potent anti-tumor activity

Yongfei Yang[1], Shuzhen Cao[1], Wenjiao Zhang[1], Jing Zhang[1], Zhe Shao[2], Xueyuan Jiang[1], Maopeng Tian[1], Luke (Zhaoxue) Yu[1]

[1]Biocytogen Pharmaceuticals (Beijing) Co., Ltd., Beijing, China; [2]Dragonboat Biopharmaceutical, Shanghai, China

biocytogen.com | info@biocytogen.com

## INTRODUCTION

The recognition of TNFR2 as a highly expressed receptor on T-cells and tumor cells makes it as an attractive target for cancer immunotherapy. A non-blocking anti-human TNFR2 antibody (BCG003) was generated from RenMab™ mice (humanized IgG mice), which is a highly effective platform for fully human antibody generation. BCG003 was selected from a large panel of antibody candidates through an unbiased, high-throughput *in vivo* efficacy screen in syngeneic tumor mouse models in humanized TNFR2 mice. BCG003 effectively promoted the proliferation of $CD8^+$ cytotoxic T cells and exerted ADCC effects on TNFR2-positive cells *in vitro*. Evaluation of anti-tumor activity of BCG003 in syngeneic mouse tumor models demonstrates that BCG003 monotherapy significantly inhibited tumor growth in a dose-dependent manner in TNFR2 humanized mice. In combination with anti-PD-1 or PD-L1 antibody, BCG003 also robustly increased antitumor activity compared to the monotherapy of each therapeutic agent. In addition, BCG003 treatment significantly increased the ratio of Teff/Treg in the TME. Importantly, BCG003 was well tolerated in TNFR2 humanized mice, with no side effects observed even when the dose was increased to 100 mg/kg. Taken together, our data demonstrates that BCG003 is a novel anti-TNFR2 antibody with potential for anti-tumor immunotherapy.

## BCG003 binds to the CRD3 and CRD4 domains of TNFR2

**BCG003 recognizes specific domains of TNFR2. A.** Cells expressing TNFR2 membrane antigen lacking different structural domains were assessed for BCG003 binding activity using flow cytometry. While BCG003 can bind to cells that express constructs lacking structural domains 1 and 2 (CRD1/CRD2) of TNFR2, BCG003 does not bind to cells that express constructs lacking structural domain 3 or 4 (CRD3/CRD4) of TNFR2. **B.** This data suggests that BCG003 binds to CRD3 and CRD4 of TNFR2.





## BCG003 exhibits Fc receptor binding ability similar to hIgG1

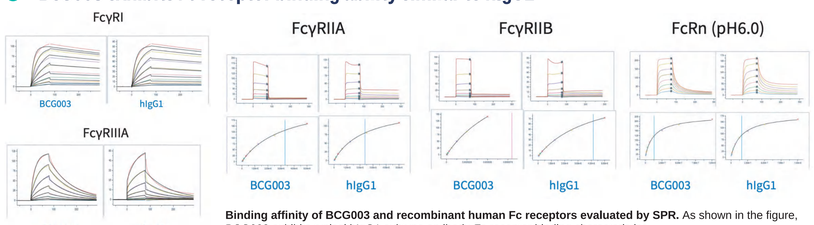


**Binding affinity of BCG003 and recombinant human Fc receptors evaluated by SPR.** As shown in the figure, BCG003 exhibits typical hIgG1 subtype antibody-Fc receptor binding characteristics.

## BCG003 binding is specific to TNFR2

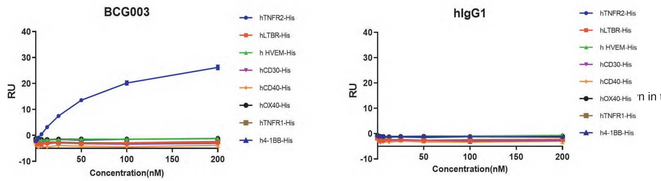


**Binding activity of BCG003 with members of TNFR family by SPR.** BCG003 could produce obvious binding signals with recombinant human TNFR2 in a concentration-dependent manner. In contrast, the response curves of BCG003 to recombinant human CD40, OX40, 4-1BB, HVEM, CD30 and TNFR1 were close to baseline.

## BCG003 has similar binding affinity to human and monkey TNFR2 recombinant proteins

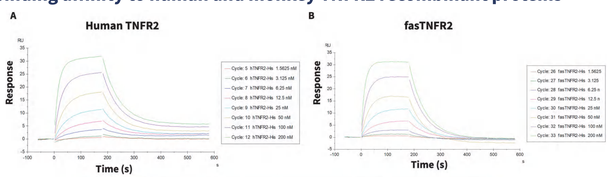


**A-B. Binding affinity of BCG003 with recombinant human and cynomolgus monkey TNFR2 by SPR.** BCG003 can bind both recombinant human and cynomolgus monkey TNFR2, with affinities at the $10^{-8}$ M level.

| Analyte 1 Solution | ka(1/Ms) | kd(1/s) | KD(M) |
|---|---|---|---|
| hTNFR2 | $2.51\times10^{5}$ | $9.40\times10^{-3}$ | $3.74\times10^{-8}$ |
| fasTNFR2 | $2.67\times10^{5}$ | $1.92\times10^{-2}$ | $7.20\times10^{-8}$ |

## BCG003 is a non-blocking TNFα antibody and displayed binding activity that is enhanced when crosslinked with FcγIIB

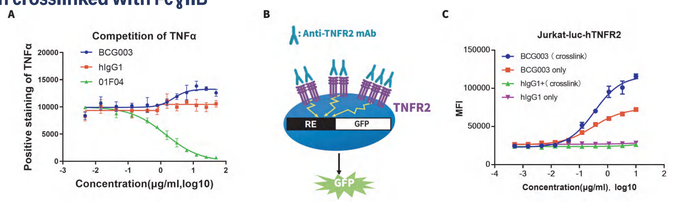


**A. BCG003 does not block binding between recombinant human TNFα and cellular TNFR2, as assessed by flow cytometry.** In this experiment, hIgG1 served as a negative homologous control, while 01F04, an antibody against TNFR2, served as a positive control.
**B-C. BCG003-mediated activation of NF-κB signaling. B.** Schematic of Jurkat-Luc-TNFR2 reporter cells. **C.** BCG003 can activate its downstream NF-κB signaling pathway by binding to TNFR2 expressed on the cell surface, exerting biological activity (red); in the presence of CHO-K1-FcγRIIB helper cells (blue), the activation effect of BCG003 is significantly enhanced compared to the non-crosslinked state.

## BCG003 has a strong ADCC effect on TNFR2-expressing cells

**ADCC activity of BCG003 antibody *in vitro*.** Cytotoxicity was evaluated using FcR-TANK as effector cells and B-hTNFR2 MC38#6-D05 (which overexpress hTNFR2) as target cells. Upon adding different concentrations of BCG003 or human IgG1 (Isotype control), the killing effect of target cells was reflected by detecting LDH in culture supernatant. The results demonstrate that BCG003 induced ADCC activity on TNFR2 positive cells.

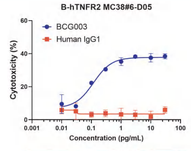


| | BCG003 | Human IgG1 |
|---|---|---|
| $EC_{50}$ (μg/mL) | 0.1176 | NA |
| R square | 0.9567 | NA |

## BCG003 stimulates the proliferation and activation of hCD8⁺ T cells and reverses $T_{reg}$ suppression

**BCG003 stimulation of hCD8 Proliferation.** A. The proliferation of human $CD8^+$ T cells was increased by hCD3 antibody in a concentration-dependent manner (accompanied by 1ug/mL hCD28 Ab stimulation). When BCG003 antibody was added (10μg/mL), the proliferation of $hCD8^+$ T cell proliferation was further stimulated. B-D. BCG003 Stimulates Proliferation and Activation of $hCD8^+$ T cells *in vitro*. After co-incubation of $hCD8^+$ T cells (with 5μg/mL OKT3 + 1μg/mL anti-CD28) and the test articles for 72h, flow cytometry was used to detect cell proliferation and release of IL-2 and IFN-γ (C-D) in the cell culture medium. The results showed that BCG003 could stimulate the proliferation (B) and activation (C-D) of $hCD8^+$ T cells. E. PBMC $CD8^+$ T cells proliferated significantly (94.8%) after stimulation with 5ng/mL hCD3 Ab and 0.1 ng/mL IL-2 for 120 h. When Treg cells (1:1) were co-cultured (1:1) with $CD8^+$ T cells, the proliferation of $CD8^+$ T cells was inhibited (reduced to about 72.4%). In contrast, BCG003 could effectively restore $CD8^+$ T cell proliferation (83.2%), but the control IgG1 antibody could not. TNFR2-HFB3: TNFR2 agonist antibody (developed by HIFIBIO). Error bars indicate SD. Significance was determined by one-way ANOVA followed by Dunnett's test. *P < 0.05, **P < 0.01.

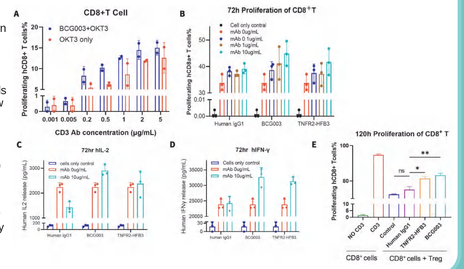


## Anti-tumor efficacy of BCG003 in MC38 and GL261 models

**Dose-dependent antitumor activity of BGC003 in the MC38 and GL261 tumor models subcutaneously inoculated in humanized B-hTNFR2 mice (i.p., biwx6).** Tumor volume growth curves of each group of mice after administration (A), and tumor volumes of each group at the end point (Day 25) (B) Error bars indicate SD.

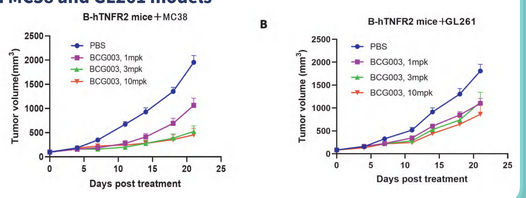


## Treatment with BCG003 enhances the efficacy of anti-PD1/PD-L1 in syngeneic tumor models

**Combination therapy of BCG003 *in vivo*.** BCG003 (i.p., biw x 6) combined with either anti-PD1 (A) or (B) anti-PD-L1 improves anti-tumor efficacy in MC38 or B16F10-hPDL1 tumors inoculated into humanized B-hTNFR2 mice. Error bars indicate SD.

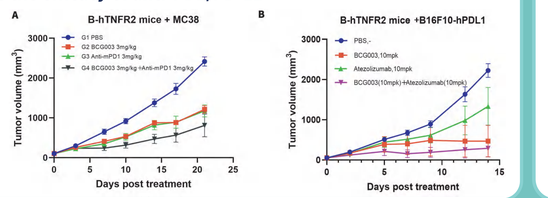


## BCG003 increases the ratio of CTL/$T_{reg}$ in TILs

**Analysis of TILs in MC38 tumors injected subcutaneously in B-hTNFR2 mice (i.p., 3mpk, biw × 4).** At the end of the experiment, flow cytometry was used to detect the proportion of infiltrated lymphocytes in each mouse tumor. The results indicate that $CD8^+$T cells were significantly increased and Treg ratio was obviously increased in BCG003 treatment group, and CTL/Treg ratio was also significantly improved. Error bars indicate SD.

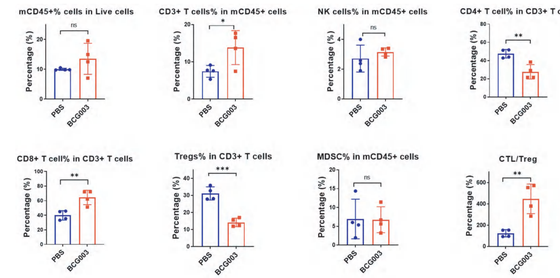


## BCG003 exhibits favorable PK characteristics in B-hTNFR2 mice

**Pharmacokinetic assessments of BCG003 *in vivo*.** Humanized B-hTNFR2 mice were injected with a single dose (i.v.) of BCG003 (10mg/kg). Blood was sampled after 15 min, 6 hr, 24 hr, and on day 3, day 5, and day 7.

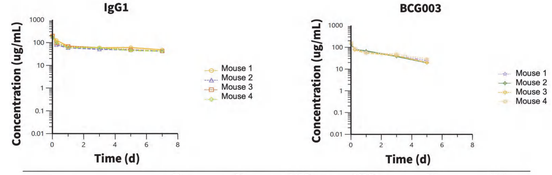


| Group | | $T_{1/2}$ (day) | $C_{max}$ (ug/mL) | $AUC_{0\text{-}last}$ (day*ug/mL) | $AUC_{0\text{-}INF}$ (day*ug/mL) | CL (mL/day/kg) | Vd (mL/Kg ) |
|---|---|---|---|---|---|---|---|
| G1 IgG1 | MEAN | 11.05 | 185.95 | 418.90 | 1115.60 | 9.13 | 142.57 |
| | CV | 18.9% | 5.2% | 8.8% | 15.7% | 15.3% | 9.2% |
| G2 BCG003 | MEAN | 2.99 | 152.90 | 250.93 | 353.43 | 28.85 | 120.63 |
| | CV | 26.3% | 5.4% | 5.4% | 16.8% | 15.3% | 10.7% |

## BCG003 does not cause toxicity in B-hTNFR2 mice at a dose of 100 mg/kg

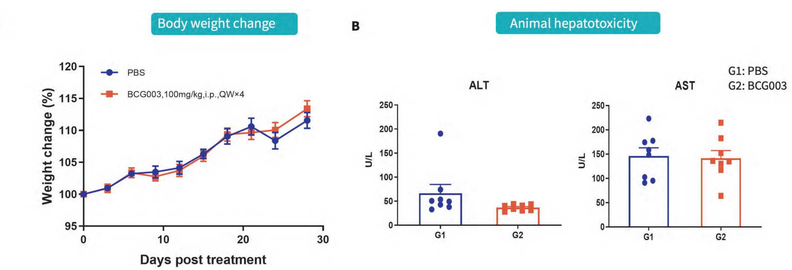


**Toxicity assessments of BDG003. A.** Body weight assessments after BCG003 administration (100 mg/kg, i.p., QW×4) to humanized B-hTNFR2 mice (n=8). No significant change was detected after treatment. **B.** Measurements of ALT and AST suggest that no hepatotoxicity was induced after administration. Error bars indicate SD.

## CONCLUSIONS & FUTURE DIRECTIONS

- BCG003 binds to the CRD3 and CRD4 domains of TNFR2 without blocking the binding of TNFα.
- *In vitro*, BCG003 stimulates the proliferation and activation of $hCD8^+$ T cells, displays ADCC effects on TNFR2–positive cells, and reverses Treg suppression of $CD8^+$ cell proliferation.
- BCG003 monotherapy demonstrates anti-tumor activity and enhances tumor inhibition efficacy in combination with anti-PD-1/PD-L1 antibodies. No toxicity was observed in hTNFR2 mice.
- Nonclinical toxicological pharmacokinetics studies in cynomolgus monkeys are ongoing, and preliminary data suggest good PK and tolerance of BCG003 in cynomolgus monkeys.

1528

# Novel preclinical candidates targeting B7-H3, 6B5 and 10F7, are suitable for development into various drug modalities

Jiangmei Li[1] , Yunyun Chen[2] , Ting Mao[2] , Peiran Li[2] , Li Hui[2], W. Frank An[2], Yanan Guo[2] , Yi Yang[2], Wenqi Hu[1] , Feng Li[1]

[1] Beijing Mabworks Biotech Co., Ltd; [2] Biocytogen Pharmaceuticals (Beijing) Co., Ltd

biocytogen.com | info@biocytogen.com

## INTRODUCTION

B7-H3 (CD276) is a type I transmembrane protein belonging to the B7 family of immune-regulatory ligands. Initially reported as a costimulatory signal of human T cells, increasing evidence suggests that it may also have coinhibitory function. TLT-2 has been identified as a potential cognate receptor for B7-H3, but others may exist. Overexpression of B7-H3 protein is found in a variety of human cancers, including lung adenocarcinomas, neuroblastomas, gliomas, and pancreatic tumors—and is associated with poor prognosis and survival. While B7-H3 can promote T cell activation and anti-tumor responses in the context of CD3 stimulation, its coinhibitory function inhibits T and NK cell activity in the tumor microenvironment.

We generated clone 6B5, a fully-human monoclonal antibody of B7-H3 from B7-H3 knock-out RenMab™ mice, which carry the complete human immunoglobulin heavy chain and kappa light chain variable regions, and its defucosylated form 6B5-AF, produced without fucose in CHO-AF cells. 6B5 binds human and monkey B7-H3 4Ig with similar affinity, which is also similar to that of enoblituzumab analog produced in house. Epitope grouping revealed different epitopes for 6B5 and enoblituzumab binding. 6B5 displays more selective binding to tumor cells and lower binding capacity toward human DC cells than reference antibodies such as enoblituzumab analog. 6B5 also showed no staining on normal human tissues. 6B5-AF demonstrated robust antibody-dependent cellular cytotoxicity (ADCC) against NCI-H520 squamous carcinoma cells without exhibiting hook effect, whereas enoblituzumab showed hook effect. 6B5 showed modest and comparable in vivo anti-tumor activity to enoblituzumab in humanized B7-H3 mice bearing murine EL4 lymphomas.

Additional anti-human B7H3 clones were also generated. The clone 10F7 showed higher endocytosis activity than DS-7300 analog in NCI-H520 cells. Both 6B5 and 10F7 showed good developability (data not shown). CMC cell lines development for 6B5 and 10F7 clones are completed. Taken together, these data suggest 6B5 and 10F7 are promising preclinical candidates for various drug modalities targeting B7H3.

References:

[1] Zhou, W. T., & Jin, W. L. (2021). B7-H3/CD276: An Emerging Cancer Immunotherapy. Frontiers in immunology, 12, 701006.

[2] Zhang, Z., Jiang, C., Liu, Z., Yang, M., Tang, X., Wang, Y., Zheng, M., Huang, J., Zhong, K., Zhao, S., Tang, M., Zhou, T., Yang, H., Guo, G., Zhou, L., Xu, J., & Tong, A. (2020). B7-H3-Targeted CAR-T Cells Exhibit Potent Antitumor Effects on Hematologic and Solid Tumors. Molecular therapy oncolytics, 17, 180–189.

## 6B5 binds a distinct epitope of B7-H3 with high binding affinity

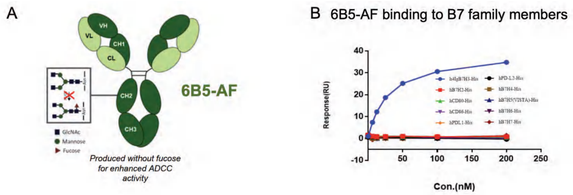


C Affinity to human/cynomolgus/mouse B7H3

| Capture | Species | ka (1/Ms) | kd (1/s) | KD (M) |
|---|---|---|---|---|
| 6B5 | Human 2Ig | 1.27E+05 | 6.53E-03 | 5.15E-08 |
| | Human 4Ig | 2.47E+05 | 3.10E-04 | 1.26E-09 |
| | Cynomolgus monkey | 2.58E+05 | 2.95E-04 | 1.14E-09 |
| | Mouse | 5.83E+04 | 1.59E-02 | 2.74E-07 |
| Enoblituzumab analog | Human 2Ig | 7.37E+04 | 2.03E-02 | 2.75E-07 |
| | Human 4Ig | 2.16E+05 | 2.39E-04 | 1.11E-09 |
| | Cynomolgus monkey | 2.31E+05 | 2.23E-04 | 9.66E-10 |
| | Mouse | No binding | No binding | No binding |

D 6B5 binds a distinct epitope compared to enoblituzumab analog and 10D7

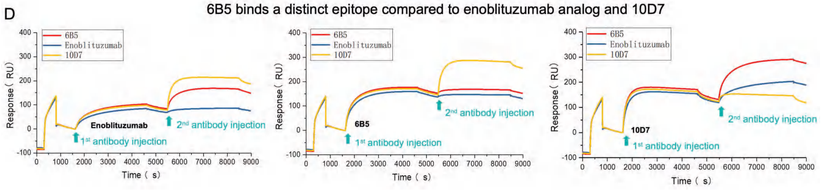


**Figure 1. Binding of 6B5.**
(A) 6B5 was generated using RenMab™ fully human antibody mice in which murine B7-H3 was knocked out. 6B5-AF was produced without fucose in CHO-AF cells. (B) 6B5 specifically binds to human B7-H3 but not other B7 family members. (C) 6B5 binding KDs. 6B5 bound human B7-H3 4Ig with comparable binding affinity to that of enoblituzumab analog, but demonstrated higher binding affinity for human B7-H3 2Ig than enoblituzumab analog. (D) 6B5 recognized a different epitope than enoblituzumab analog or another clone 10D7.

## 6B5 binds selectively to B7-H3 positive tumor cells, unlike reference antibodies

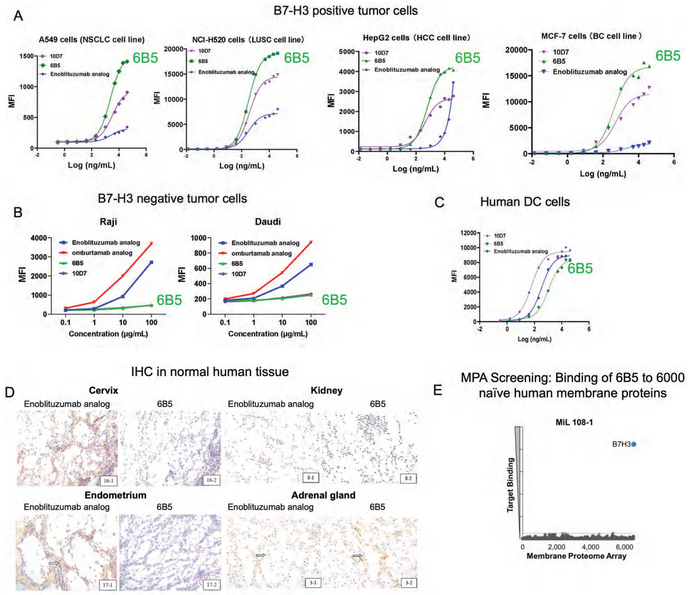


**Figure 2. 6B5 binds selectively to B7-H3 positive tumor cells, unlike reference antibodies.**
6B5 bound B7-H3 positive tumor cell lines with higher capacity than reference antibodies (A) but did not bind B7-H3 negative tumor cell lines, unlike certain reference antibodies (B). 6B5 binding to human DC was less than reference antibodies too (C). 6B5 shows minimal staining of human normal tissues, cleaner than reference antibody enoblituzumab analog, by immunohistochemistry (IHC) (D). 6B5 shows highly specific binding to B7-H3, but not other human membrane proteins by membrane proteome array (MPA) screening (E).

## 6B5-AF induces robust ADCC without hook effect

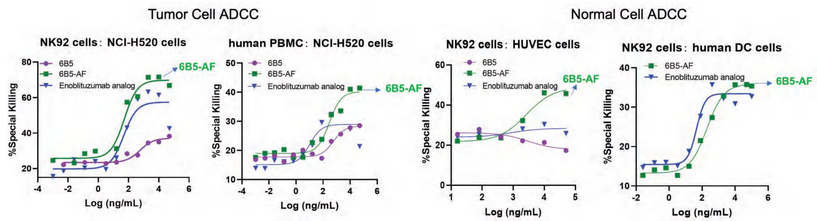


**Figure 3. 6B5-AF induced antibody-dependent cellular cytotoxicity (ADCC) against tumor cells *in vitro*.**
ADCC activities of 6B5-AF, 6B5, and enoblituzumab analog were measured by flow cytometry. 6B5-AF exhibited robust ADCC against NCI-H520 tumor cells with similar (NK92) or stronger activities than reference antibody enoblituzumab. Further, 6B5-AF-mediated ADCC showed no hook effect against NCI-H520 cells, in contrast to enoblituzumab analog. 6B5-AF also induced ADCC against normal human cells, with moderately weaker potency against DC cells, and stronger potency in HUVEC cells relative to enoblituzumab analog.

## Anti-tumor activity of 6B5-AF in a syngeneic mouse model

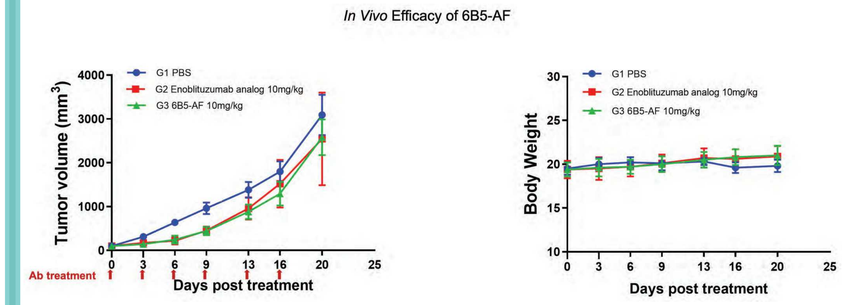


**Figure 4. 6B5-AF elicits comparable anti-tumor activity to enoblituzumab analog in a syngeneic mouse model.**
6B5 delayed tumor growth in humanized B7-H3 mice inoculated SC with the mouse cell line EL-4 overexpressing human B7-H3 (EL-4-hB7-H3), without impacting body weight.

## Anti-human B7-H3 clone 10F7 induces robust internalization activity

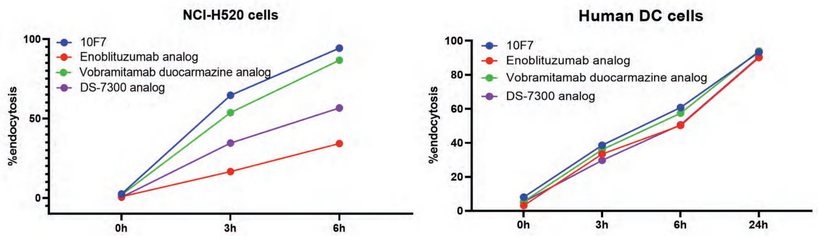


**Figure 5. Internalization of B7-H3 clone 10F7.**
10F7 induced stronger internalization activity than reference antibodies in NCI-H520 cells, but showed similar activity in DC cells.

## CONCLUSIONS

**6B5 and 10F7, two anti-human B7-H3 clones, are preclinical candidates suitable for different modalities of B7-H3-targeted therapies.**

- 6B5 is a high affinity, highly B7-H3-selective, fully human antibody with a distinct binding epitope.
- 6B5 binds selectively to B7-H3 positive tumor cells with clean normal tissue staining by IHC, unlike reference antibodies.
- 6B5-AF shows robust ADCC without the hook effect. It demonstrates modest anti-tumor activity in a syngeneic mouse model.
- 10F7 demonstrates superior internalization activity compared with reference antibodies, which is suitable for ADC discovery.
- Both 6B5 and 10F7 have excellent developability. CMC development is underway with cell lines generated.

6435

# BCG008, a human SIGLEC-15 blocking antibody, displays potent anti-tumor activity in SIGLEC-15-humanized mice

Yongfei Yang[1], Aidong Qu[2], Fengping Yao[1], Pan Song[1], Hongyuan Liang[2], Maopeng Tian[1], Fang Yang[1], Zhaoxue Yu[1], Xu Zhou[2], Xiuling Li[2]

[1]Biocytogen Pharmaceuticals (Beijing) Co., Ltd., Beijing, China; [2]Shanghai Institute of Biological Products Co., Ltd, Shanghai, China

## INTRODUCTION

Sialic acid-binding Ig-like lectin 15, or SIGLEC-15, is identified as a critical immune suppressor. SIGLEC-15 expression is normally limited to certain myeloid cells, but it can be upregulated in a variety of tumors and on tumor-infiltrating myeloid cells. SIGLEC-15 significantly inhibits antigen-specific T cell responses both *in vitro* and *in vivo*. Conversely, genetic ablation of SIGLEC-15 promotes anti-tumor responses. Therefore, a SIGLEC-15-targeting blocking antibody could represent a novel class of anti-tumor immunotherapy.

BCG008, a fully human monoclonal antibody antagonist of SIGLEC-15, was generated from RenMab™ mice, which contain the entire human immunoglobulin variable domain. Compared to a reference SIGLEC-15 blocking antibody (5G12), BCG008 exhibited higher affinity for human and cynomolgus monkey SIGLEC-15 and recognized a different binding epitope. In *in vitro* studies, BCG008 significantly abrogated SIGLEC-15-mediated T cell suppression in a dose dependent manner, as measured by $CD4^+$ and $CD8^+$ T cell proliferation. Subsequently, the efficacy and safety of BCG008 was evaluated in syngeneic tumor models in SIGLEC15-humanized mice. BCG008 monotherapy significantly inhibited tumor growth, and the effect of the tumor inhibition was potentiated when administered in combination with immune-checkpoint inhibitors, including anti-human PD-L1 antibody and anti-human 4-1BB antibody in syngeneic tumor models in humanized mice. In safety evaluation, BCG008 was well-tolerated in the tumor-bearing mice; no adverse effects were observed even at high doses (e.g. 30 mg/kg). Taken together, these results demonstrate that BCG008 is a novel anti-human SIGLEC-15 blocking antibody with favorable efficacy and safety profiles that can provide potential benefits for future cancer immunotherapy.

## BCG008 has high affinity for hSIGLEC-15 and fasSIGLEC-15

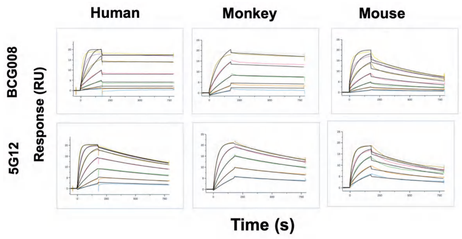


| | | ka (1/Ms) | kd (1/s) | KD (M) |
|---|---|---|---|---|
| BCG008 | hSIG-15-His | 4.19E+06 | 6.85E-07 | 1.64E-13 |
| | fasSIG-15-His | 8.22E+05 | 1.67E-04 | 2.04E-10 |
| | mSIG-15-His | 6.39E+05 | 1.26E-03 | 1.97E-09 |
| 5G12 | hSIG-15-His | 2.93E+06 | 8.56E-04 | 2.92E-10 |
| | fasSIG-15-His | 2.62E+06 | 7.50E-04 | 2.86E-10 |
| | mSIG-15-His | 2.85E+06 | 1.18E-03 | 4.13E-10 |

**Binding affinity of BCG008 to human, cynomolgus monkey, and mouse SIGLEC-15 by SPR.** BCG008 can bind all SIGLEC-15 proteins, with high affinity at the $10^{-9}$ M level.

## BCG008 recognizes a different SIGLEC-15 epitope when compared to 5G12

**Biolayer interferometry (BLI) molecular interaction assay (left) and epitope binding assessments from BLI molecular interaction assay (right).** The higher signal suggests that BCG008 and reference antibody 5G12 bind different epitopes of the SIGLEC-15 protein and do not compete with one another.

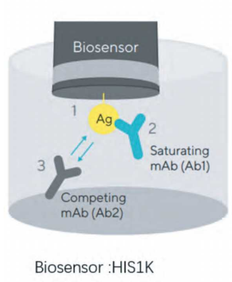


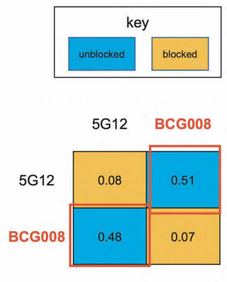


## BCG008 reverses SIGLEC-15 mediated T cell suppression in a dose-dependent manner

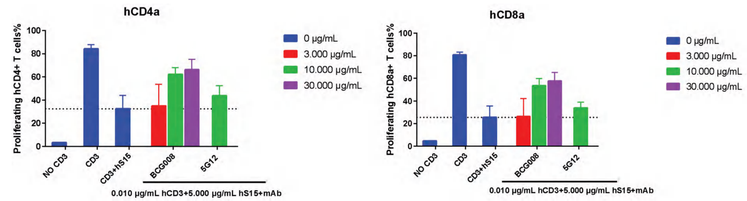


**In culture, BCG008 can relieve the inhibition of CD4 and CD8 T cell proliferation caused by hSIGLEC-15 protein (CD3 + hS15) in a dose-dependent manner.** Error bars indicate SD.

## BCG008 exhibits strong tumor suppressive effects

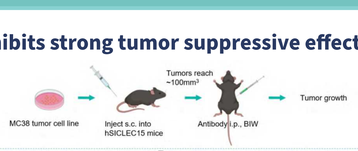


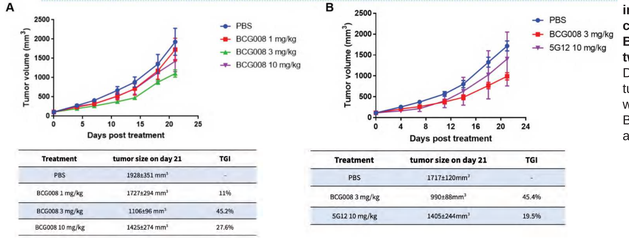


| Treatment | tumor size on day 21 | TGI |
|---|---|---|
| PBS | 1928±351 mm³ | - |
| BCG008 1 mg/kg | 1727±294 mm³ | 11% |
| BCG008 3 mg/kg | 1106±96 mm³ | 45.2% |
| BCG008 10 mg/kg | 1425±274 mm³ | 27.6% |

| Treatment | tumor size on day 21 | TGI |
|---|---|---|
| PBS | 1717±120mm³ | - |
| BCG008 3 mg/kg | 990±86mm³ | 45.4% |
| 5G12 10 mg/kg | 1405±244mm³ | 19.5% |

**Humanized B-hSIGLEC-15 mice were subcutaneously injected with MC38 tumor cells and treated with BCG008 as a single agent twice a week as indicated.** A. Dose-responsive inhibition of tumor growth. B. Compared with reference antibody, BCG008 exhibits a stronger antitumor effect.

## BCG008 combination therapies enhance anti-tumor efficacy


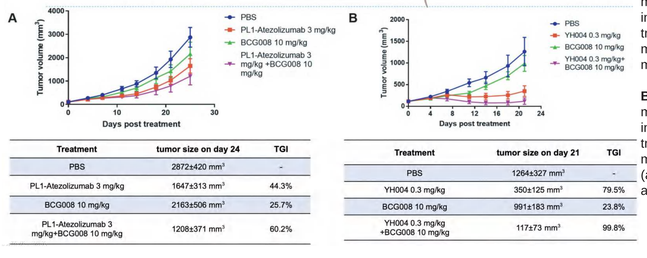


| Treatment | tumor size on day 24 | TGI |
|---|---|---|
| PBS | 2872±420 mm³ | - |
| PL1-Atezolizumab 3 mg/kg | 1647±313 mm³ | 44.3% |
| BCG008 10 mg/kg | 2163±506 mm³ | 25.7% |
| PL1-Atezolizumab 3 mg/kg+BCG008 10 mg/kg | 1208±371 mm³ | 60.2% |

| Treatment | tumor size on day 21 | TGI |
|---|---|---|
| PBS | 1264±327 mm³ | - |
| YH004 0.3 mg/kg | 350±125 mm³ | 79.5% |
| BCG008 10 mg/kg | 991±183 mm³ | 23.8% |
| YH004 0.3 mg/kg +BCG008 10 mg/kg | 117±73 mm³ | 99.8% |

**A.** Humanized hSIGLEC-15 mice were subcutaneously injected with MC38 cells and treated with BCG008 10 mg/kg and anti-PD-L1 (3 mg/kg) twice a week.

**B.** Humanized B-h4-1BB mice were subcutaneously injected with MC38 cells and treated with BCG008 10 mg/kg and YH004 (anti-4-1BB; 0.3 mg/kg) twice a week.

## BCG008 has an extended half-life in B-hSIGLEC-15 mice compared to 5G12

BCG008; $T_{1/2}$=9.79 days

5G12; $T_{1/2}$=4.52 days

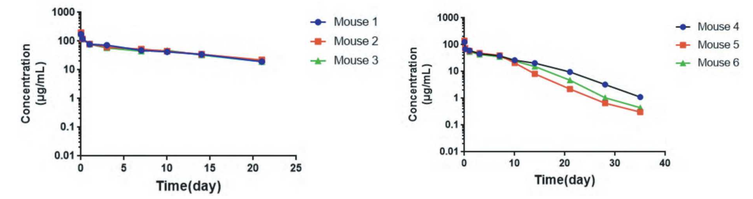


**Pharmacokinetic assessments of BCG008 *in vivo*. Humanized B-hSIGLEC-15 mice were injected with a single dose (i.v.) of BCG008 (10 mg/kg).** Blood was sampled after 15 min, 4 hours, and 24 hours, and on day 3, day 7, day 10, day 14, and day 21. Results indicate a longer half-life of BCG008 *in vivo* compared to the benchmark antibody 5G12.

## BCG008 does not exhibit toxicity in B-hSIGLEC-15 mice at a dose of 30 mg/kg

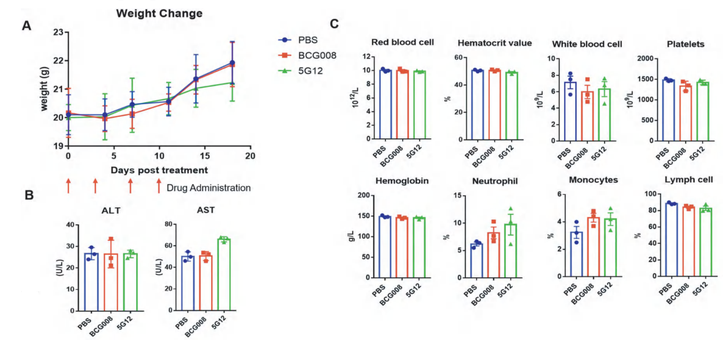


**A.** Body weight assessments after BCG008 administration to B-hSIGLEC-15 mice. No significant change was detected after treatment with BCG008 compared to PBS controls. **B-C.** Measurements of ALT, AST and CBC profiles suggest no hepatotoxicity or hematotoxicity of BCG008. Error bars indicate SD.

## CONCLUSIONS

- BCG008 is a novel, fully human anti-SIGLEC-15 antibody generated from RenMab™ mice
- BCG008 has higher hSIGLEC-15 & fasSIGLEC-15 affinity and recognizes a different epitope than 5G12
- BCG008 reverses SIGLEC-15 mediated T cell suppression in a dose-dependent manner
- BCG008 has a longer half-life than 5G12 (9.79 days vs. 4.19 days)
- BCG008 has strong antitumor efficacy and a good safety profile *in vivo*

biocytogen.com | info@biocytogen.com

2977

# A First-In-Class Anti-HER2/TROP2 Bispecific Antibody-Drug Conjugate (YH012) Exhibits Potent Anti-Tumor Efficacy

Chengzhang Shang[1], Gao An[1], Yuming Guo[1], Ellen Zhang[2], Qingcong Lin[2], Yi Yang[1]

[1] Biocytogen (Pharmaceuticals) Beijing Co., Beijing, China; [2] Biocytogen Boston Corporation, Wakefield, MA, USA

biocytogen.com | info@biocytogen.com

## ABSTRACT

Antibody-drug conjugates (ADC) are a therapeutic modality that combines the advantages of potent killing from small molecule cytotoxic payload and highly specific targeting from monoclonal antibodies. By targeting dual tumor-associated antigens (TAA), the bispecific ADC (BsADC) serves as a promising therapeutic strategy that can further increase tissue specificity and selectivity. HER2 and TROP2 are two TAAs that are commonly expressed and co-expressed by multiple tumor types, including gastric, colorectal, bladder, breast, and non-small-cell lung cancer (NSCLC). Of note, TROP2 expression has been detected in a wide range of HER2-low expressing tumors. These data led us to predict that targeting HER2 and TROP2 with a BsADC would provide therapeutic benefit, especially for patients with HER2-low cancers. Hence, we generated YH012, a first-in-class BsADC that contains a fully human bispecific anti-HER2/TROP2 antibody conjugated with monomethyl auristatin E (MMAE) via a protease-cleavable linker. In vitro, YH012 demonstrated enhanced affinity, internalization, and tumor selectivity compared to its parental monoclonal and monovalent anti-HER2 or anti-TROP2 antibodies. In vivo, YH012 showed strong anti-tumor activity in multiple cell line-derived and patient-derived xenografts (CDX and PDX) of NSCLC, gastric, pancreatic, and breast cancer. Moreover, YH012 exhibited superior anti-tumor efficacy than benchmark antibodies in both HER2-positive and HER2-low xenograft models, indicating that YH012 has a potent and broad therapeutic effect. In summary, YH012 has the advantages of increased potency, tissue specificity, and reduced toxicity as a novel BsADC that can be further exploited to treat HER2 and TROP2 co-expressing tumors, especially HER2-low tumors.

## HER2 and TROP2 are co-expressed at high levels in multiple solid tumors

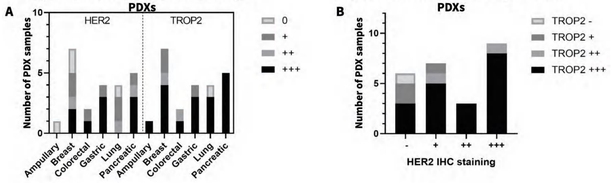


**HER2 and TROP2 (co)expression analysis in a variety of solid tumors.** We analyzed HER2 and TROP2 protein levels by immunohistochemistry (IHC) in several PDXs. Co-expression of HER2 and TROP2 has been found across several tumors including gastric, colorectal, breast, and non-small-cell lung cancers (NSCLC) (A). TROP2 expression was detected with a wide range of HER2 expression subtypes, including HER2-positive and HER2-low subtypes (B).

## HER2 and TROP2 are co-expressed at high levels in multiple solid tumors

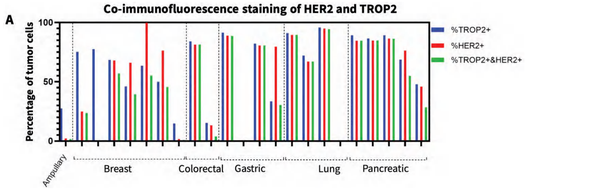


**HER2 and TROP2 (co)expression analysis in a variety of solid tumors.** We analyzed HER2 and TROP2 protein levels by immunofluorescence (IF) in several PDXs. HER2 and TROP2 levels are highly co-expressed in a variety of PDXs and shows intra-tumor heterogeneity (A, B). The numbers represent the percentage of positive tumor cells (B).

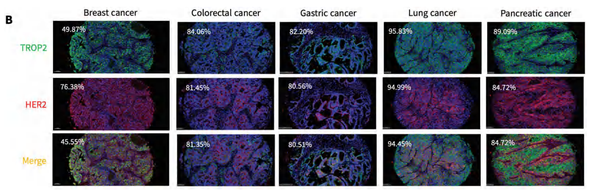


## YH012 exhibited strong dual-target binding

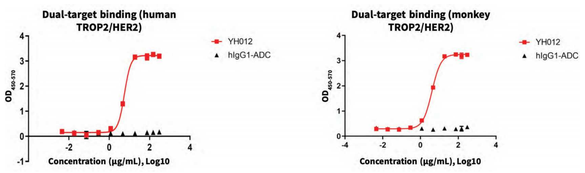


**Co-binding affinity of YH012.** 96-well plate were coated with either human or monkey TROP2, followed by adding YH012 (a bispecific anti-HER2 and TROP2 antibody-drug conjugate) samples to allow YH012 binding to the immobilized TROP2. Next, human or monkey HER2-Avitag was added and Streptavidin-HRP (enzyme) was used for detection by ELISA. YH012 displayed good co-binding affinity with HER2 and TROP2.

## YH012 exhibited strong cross-arm binding avidity

**Tumor cell line binding.** The results showed that compared to parental monovalent antibodies, YH012 (unconjugated) had a higher binding avidity in three tested cell lines (NCI-N87, NCI-H1975 and MCF-7). This suggests that the avidity provided by a single arm is insufficient for effective binding. While the YH012 (unconjugated) demonstrated strong cross-arm avidity binding as it can concurrently bind both HER2 and TROP2 antigens on the surface of the same cell.

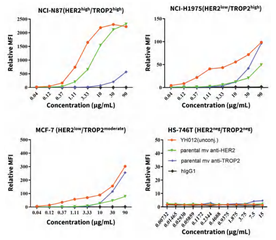


## YH012 exhibited enhanced internalization

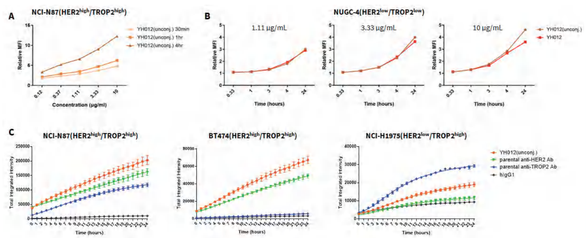


**Internalization of YH012.** Endocytosis kinetics of the unconjugated form of YH012 (unconj.) are dose-dependent and remain consistent upon conjugation, as depicted in (A, B). In NCI-N87 and BT474 cell lines, unconjugated YH012 demonstrated superior internalization compared to its parental antibodies. In addition, endocytosis of YH012 was elevated in a cell line with low HER2 (NCI-H1975) compared to its parent HER2 antibody (C).

## YH012 exhibited strong cross-arm selectivity

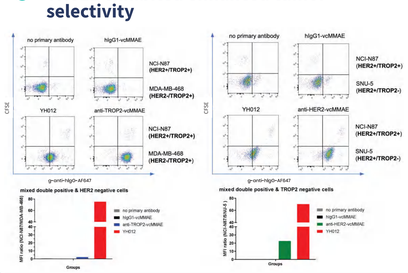


***In vitro* selectivity of YH012.** The in vitro tumor selectivity was determined by calculating the MFI ratio of double-positive NCI-N87 cells to single-positive cell line cellular binding (MFI of NCI-N87/MDA-MB-468 or SNU-5). NCI-N87 and MDA-MB-468/SNU-5 cells were mixed in a ratio of 1:10. YH012 preferentially binds double-positive NCI-N87 cells over tumor cells that express single target TROP2 or HER2, demonstrated higher selectivity compared with the parental ADCs. This enhanced tumor selectivity is indicative of a strong avidity mediated by cross-binding of HER2 and TROP2 antigens on double-positive tumors.

## YH012 showed increased *in vivo* anti-tumor activity

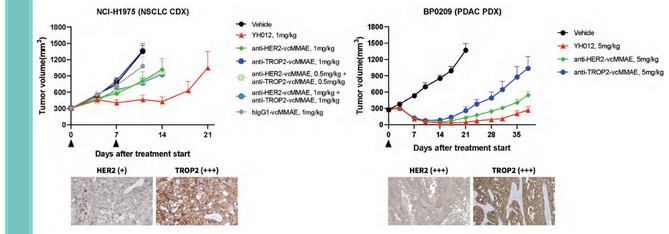


***In vivo* anti-tumor activity of YH012 in xenograft tumor models.** YH012 exhibitied increased anti-tumor activity in both cell line-derived xenograft (CDX, NSCLC) and patient derived xenograft (PDX, PDAC) models compared with parental HER2 and TROP2 antibody-drug conjugates.

## YH012 showed superior anti-tumor efficacy in both HER2-positive and HER2-low xenograft models

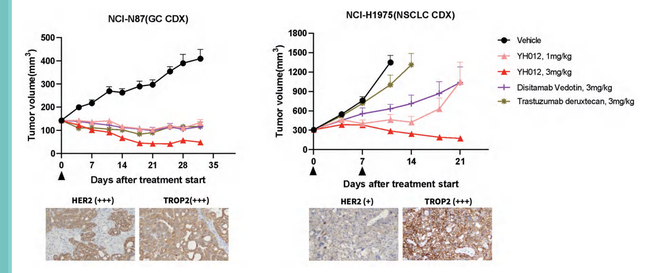


***In vivo* anti-tumor activity of YH012 in HER2-positive and HER2-low CDX models.** YH012 showed superior efficacy compared with HER2 benchmark ADCs in both HER2-positive and HER2-low CDX models.

## YH012 showed potent anti-tumor activity in HER2-low PDX models

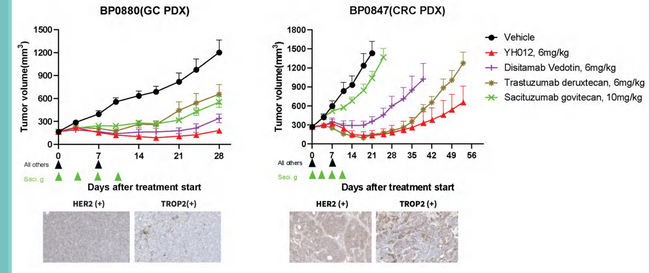


***In vivo* anti-tumor activity of YH012 in HER2-low PDX models.** YH012 showed potent anti-tumor activity in HER2-low gastric and colorectal cancer PDX models.

## YH012 showed potent anti-tumor activity in HER2-low PDX models

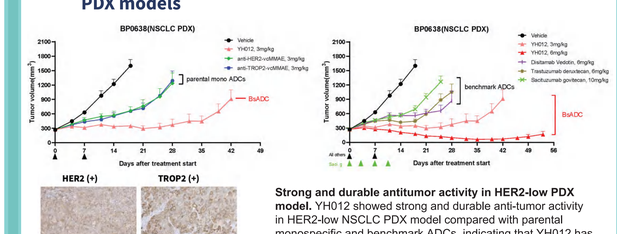


**Strong and durable antitumor activity in HER2-low PDX model.** YH012 showed strong and durable anti-tumor activity in HER2-low NSCLC PDX model compared with parental monospecific and benchmark ADCs, indicating that YH012 has strong therapeutic potential to overcome the drug resistance of single target-ADCs caused by tumor heterogeneity.

## YH012 showed effective MMAE accumulation in tumors from a CDX model

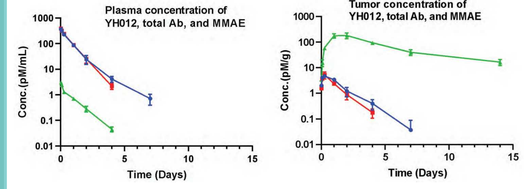


**Pharmacokinetic analysis of YH012 in NCI-H1975 xenograft model.** After a single dose of 3 mg/kg of YH012, the payload MMAE was found to accumulate in the tumor but was present at low levels in the plasma. This suggests that YH012 has reached an efficient tumor-targeted delivery of MMAE and may have better antitumor activity.

## YH012 was stable in human and monkey plasma

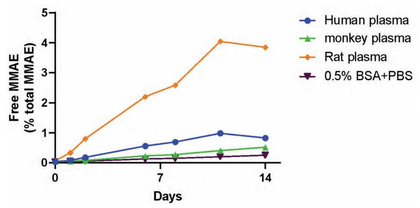


***In vitro* stability analysis of YH012 in plasma.** The release of MMAE from YH012 over 14 days at a concentration of 100 μg/mL and 37°C was evaluated in rat, monkey, and human plasma. The results showed that the release of free MMAE from YH012 was between 0.5% to 1.0% on day 14 in monkey and human plasma, indicating that YH012 remains stable in these types of plasma.

## CONCLUSIONS

- **HER2 and TROP2 are co-expressed in a wide range of tumor types. Of note, TROP2 was also expressed in many HER2-low solid tumors, such as HER2-low breast cancers, suggesting broad therapeutic indications of YH012.**
- **YH012 demonstrated superior internalization compared to its parental monospecific Abs.**
- **YH012 was shown to increase tumor cell specificity and minimize side effects in normal cells.**
- **YH012 showed increased anti-tumor activity in both HER2-high and HER2-low CDX and PDX models, as well as durable efficacy than benchmarks, indicating that YH012 has strong therapeutic potential, especially in HER2-low expressing cancers.**
- **By targeting dual TAAs, YH012 has the potential to increase tumor specificity and potency, reduce toxicity, and overcome tumor heterogeneity.**
- **The backbone of YH012 molecule is constructed using RenLite plus knobs-into-holes technology, offering excellent BsAb assembly efficiency, good physicochemical properties and CMC developability.**

2978

# YH013, a Novel EGFR x MET Bispecific Antibody-Drug Conjugate, Exhibits Potent Anti-Tumor Efficacy


Yanfei Han[1], Chengzhang Shang[1], Zhuolin Li[1], Zhenyan Han[1], Jun Li[1], Zixu Cui[1], Gao An[1], Wanjun Hao[1], Yujie Liu[1], Hao Li[1], Baihong Liu[1], Ellen Zhang[2], Qingcong Lin[2], Yi Yang[1], Yuelei Shen[1]

[1]Biocytogen Pharmaceuticals (Beijing) Co., Ltd., Beijing, China; [2]Biocytogen Boston Corporation, Wakefield, MA, USA

biocytogen.com | info@biocytogen.com



## ABSTRACT

Bispecific antibodies (BsAb) that target dual tumor-associated antigens have the advantages of invoking synergistic effects between two signaling pathways, increasing target tissue specificity, and reducing systemic toxicity. By combining the antibody-mediated specific targeting with potent killing from a cytotoxic payload, antibody-drug conjugates (ADC), and especially bispecific ADCs (BsADC), have become powerful therapeutic strategies. EGFR and MET are oncogenic proteins that are co-expressed in a wide range of tumors. Moreover, MET amplification is largely associated with drug resistance of EGFR tyrosine kinase inhibitors in non-small cell lung cancer (NSCLC) patients. Biocytogen developed a fully human EGFR x MET BsADC using our proprietary common light chain RenLite® mouse platform and knobs-into-holes technology. The BsAb showed enhanced internalization and binding affinity compared to parental monoclonal and monovalent antibodies in the EGFR/MET co-expressing NCI-H1975 cell line. After conjugating the BsAb with monomethyl auristatin E (MMAE) via a protease-cleavable linker, the resulting BsADC, YH013, exhibited a remarkable and dose-dependent anti-tumor efficacy in NCI-H1975 and NCI-H292 cell line-derived xenograft models. Moreover, in multiple patient-derived xenografts of NSCLC and pancreatic ductal adenocarcinoma (PDAC), which co-express EGFR and MET, YH013 demonstrated superior and durable efficacy that outperformed benchmark antibodies at a lower dose (3 mg/kg). Collectively, these results suggest that YH013 can be an effective treatment option for EGFR and MET co-expressing tumors and overcome MET-driven EGFR-TKI resistance to improve patient outcomes.


## Co-expression of EGFR/MET in multiple cancer cell lines

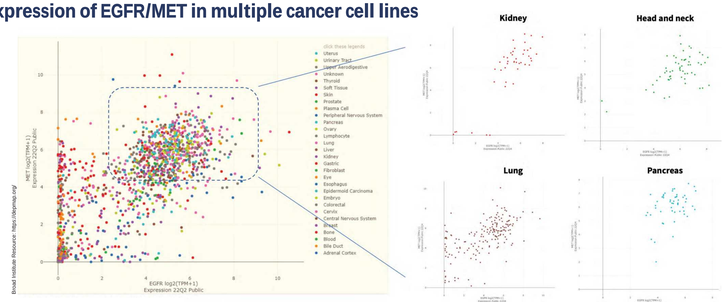


Genetic profiling of thousands of cancer cell lines (DepMap database) revealed that EGFR and MET are commonly co-expressed in multiple cancer cell lines.

## Biocytogen's RenLite® Platform-based Bispecific ADC Discovery

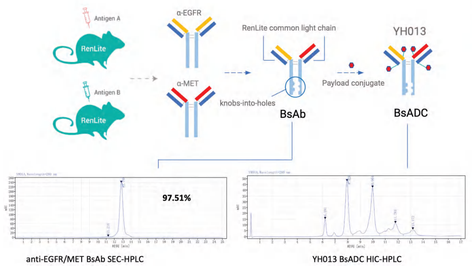


### Highlights

- **RenLite® mice with target gene knockout (Target KO-RenLite) allow to generate antibodies with increased diversity, affinity, and potentially novel epitopes.**
- **Common light chain design reduces heavy & light chain mispairing and ensures good developability.**
- **High-throughput and rapid generation of high-quality bispecific antibodies (BsAbs).**
- **Dual TAA-targeting format for development of bispecific ADCs (BsADCs).**

## EGFR and MET are co-expressed in different tumor cell lines

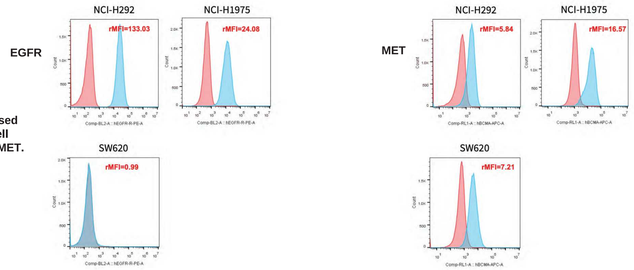


**EGFR and MET are co-expressed in NCI-H292 and NCI-H1975 cell lines. SW620 only expresses MET.**

## YH013 displayed different binding behaviors in NCI-H1975 versus NCI-H292 tumor cells

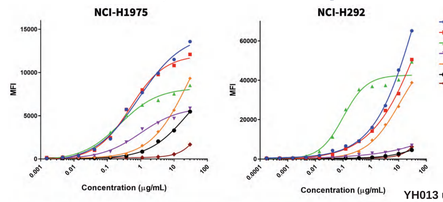


| EC50 (ug/ml) | NCI-H1975 | NCI-H292 |
|---|---|---|
| YH013 unconj. | 0.88 | 48.34 |
| YH013 | 0.4976 | 93.3 |
| anti-EGFR | 0.2465 | 0.09943 |
| anti-MET | 0.9818 | - |
| anti-EGFR/control | 25.81 | 10.98 |
| anti-MET/control | 22.09 | 63.25 |

| Cell line | EGFR mutations | EGFR amplification | MET mutations | MET amplification |
|---|---|---|---|---|
| NCI-H1975 | L858R,T790M | N | WT | N |
| NCI-H292 | WT | N | WT | N |

**YH013 unconj. showed improved binding compared to its parental Abs in NCI-H1975 cancer cells, where the expression of EGFR and MET are moderate.** In contrast, in the NCI-H292 cancer cell line, which has high expression of EGFR and moderate expression of MET, the binding ability of YH013 was weaker than that of the EGFR Ab. This suggests that the binding avidity of YH013 is provided by both the EGFR and MET arms and is dependent on the levels of EGFR and MET expressed on the same cell surface.

## YH013 unconj. displayed enhanced internalization in MET$^+$ EGFR$^+$ cancer cell line

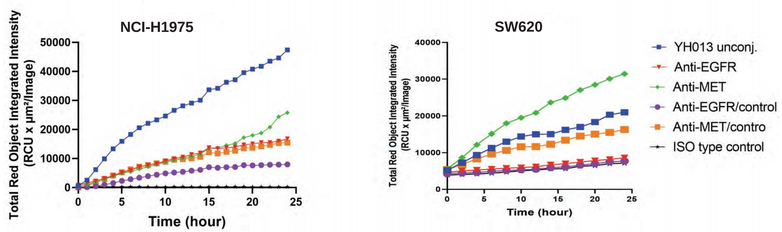


**YH013 unconj. showed enhanced internalization activity compared to its monovalent and parental mAbs in NCI-H1975 MET$^+$ EGFR$^+$ cancer cell line.** The internalization activity of YH013 unconj. was equivalent to that of its monovalent MET antibody in SW620 MET$^+$ EGFR$^-$ cell line.

## YH013 showed potent and synergistic efficacy in CDX model

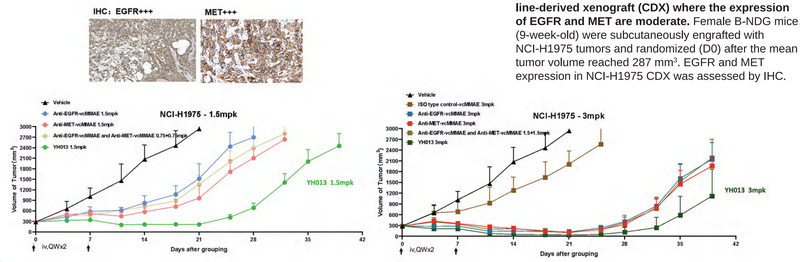


**YH013 showed robust anti-tumor efficacy than their parental monoclonal ADCs in NCI-H1975 cell line-derived xenograft (CDX) where the mean tumor volume reached 287 mm³. EGFR and MET expression in NCI-H1975 CDX was assessed by IHC.**

## YH013 inhibited tumor growth in PDX models of pancreatic cancer

**YH013 showed robust anti-tumor activity in multiple pancreatic cancer PDX models in severely immuno-deficient B-NDG mice.** Female B-NDG mice aged 6 weeks were subcutaneously implanted with PDX of BP209 or BP0226 pancreatic cancer and randomized (D0) after the mean tumor volume reached 339-340 mm³ and 293-294 mm³, respectively. EGFR and MET expression in BP0209 and BP0226 PDXs were assessed by IHC.

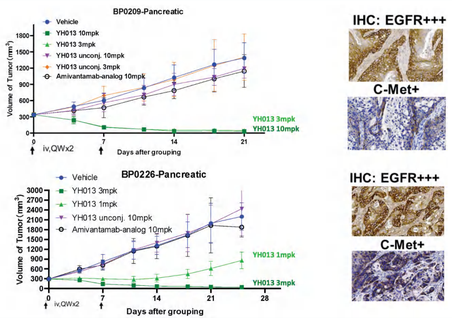





## YH013 inhibited tumor growth in PDX models of lung cancer

**YH013 showed robust anti-tumor activity in multiple Lung cancer PDX models in severely immunodeficient B-NDG mice.** Female B-NDG mice aged 5-6 weeks subcutaneously implanted with PDX of BP0101 and BP0638 lung cancer and randomized (D0) after the mean tumor volume reached 252-255 mm³ and 267 mm³, respectively. EGFR and MET expression in BP0101 and BP0638 PDXs were assessed by IHC.

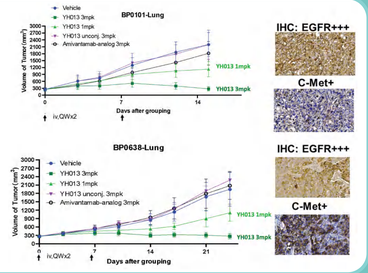


## YH013 also showed durable anti-tumor effect in CDX model of NCI-H1975 (Lung cancer) engrafted in nude mice

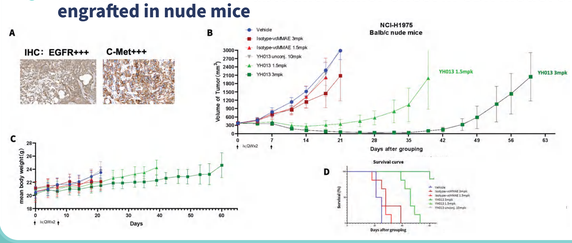


**Female nude mice aged 7-9 weeks subcutaneously implanted with NCI-H1975 tumors and randomized (D0) after the mean tumor volume reached 298 mm³.** EGFR and MET expression in NCI-H1975 CDX were assessed by IHC. (A) Representative scan of NCI-H1975 tumor section stained for EGFR and MET by IHC. (B) YH013, YH013 unconj. and isotype-vc-MMAE were administered i.v. to treatment groups of 6 mice each. (A) Vehicle-treated group served as control. (C) Mean body-weight data. (D) Survival analysis.

## YH013 showed anti-tumor effect in CDX model of NCI-H292 (lung cancer) engrafted in nude mice

**YH013 showed robust anti-tumor activity in Lung cancer PDX models in nude mice.** Female B-NDG mice aged 7-9 weeks subcutaneously implanted with CDX of NCI-H292 lung cancer and randomized (D0) after the mean tumor volume reached 311-312 mm³. EGFR and MET expression in NCI-H292 CDX were assessed by IHC.

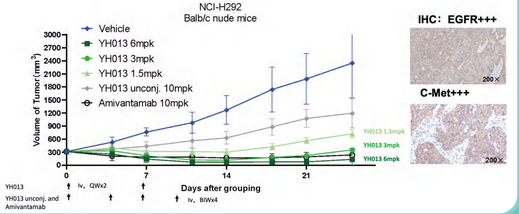


## YH013 showed robust anti-tumor effect in PDX model of BP0508 (Lung cancer) engrafted in nude mice

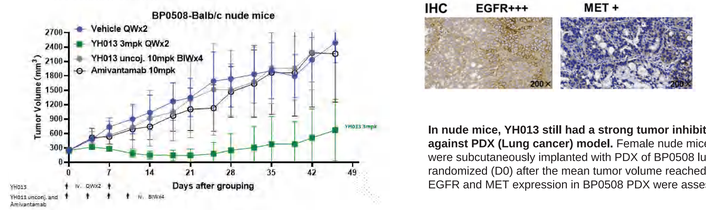


**In nude mice, YH013 still had a strong tumor inhibition effect against PDX (Lung cancer) model.** Female nude mice (6-week-old) were subcutaneously implanted with PDX of BP0508 lung cancer and randomized (D0) after the mean tumor volume reached 245 mm³. EGFR and MET expression in BP0508 PDX were assessed by IHC.

## CONCLUSIONS

- **YH013 is a novel fully-human bsADC generated from the RenLite® platform that target EGFR and c-Met, which are co-expressed in a wide range of tumor types**
- **By targeting dual TAAs, YH013 showed increased tumor cell specificity and higher internalization in EGFR/MET co-expressing tumor cells where the antibody binding capacity of EGFR and c-Met were similar**
- **The BsAb backbone of YH013 molecule is constructed using RenLite® common light chain plus knobs-into-holes (KIH) technologies allow for efficient BsAb assembly and great CMC developability**
- **YH013 showed outstanding and dose-dependent anti-tumor activity in both CDX and PDX models than benchmark antibodies at lower doses**

6325

# A novel EGFR x MUC1 bispecific antibody-drug conjugate, BSA01, targets post-cleavage membrane bound MUC1-C and improves tumor selectivity


Yifu Zhang[1], Chengzhang Shang[1], Anqi Wang[1], Jia Zhang[1], Yuji Liu[1], Hao Li[1], Xiaopeng Li[1], Gao An[1], Li Hui[2], W. Frank An[1], Yi Yang[1]

[1]Biocytogen Pharmaceuticals (Beijing) Co., Ltd., Beijing, China; [2]Biocytogen Boston Corporation, Wakefield, MA, USA

biocytogen.com | info@biocytogen.com


## INTRODUCTION

Epidermal growth factor receptor (EGFR) and mucin 1 (MUC1) are tumor-associated antigens (TAA) that are highly co-expressed in esophageal squamous cell carcinoma, non-small cell lung cancer (NSCLC), and triple negative breast cancer, among others. MUC1, a glycoprotein essential for the formation of the epithelial mucous barrier, is hypoglycosylated and dimerizes with EGFR, a potent oncoprotein, in transformed cells. Dual targeting of both TAAs represents a promising therapeutic strategy to treat the aforementioned malignancies. We generated a fully human anti-EGFRxMUC1 bispecific antibody-drug conjugate (BSA01) using the fully human, common light chain antibody transgenic mice, RenLite®. BSA01 is a regular 1+1 Y-shaped bispecific antibody conjugated with monomethyl auristatin E (MMAE). Our data suggests that the anti-MUC1 arm of BSA01 targets MUC1-C*, the C-terminal ectodomain of MUC1 which remains membrane-bound after cleavage[1]. The affinity- and internalization-optimized anti-EGFR arm aims to improve tumor selectivity and to reduce on-target skin toxicity. Internalization assays demonstrated that unconjugated BSA01 was endocytosed in tumor cells co-expressing EGFR and MUC1 more efficiently than mono- or bivalent parental antibodies targeting EGFR or MUC1. BSA01 exhibited strong cytotoxicity *in vitro* against gastric, NSCLC, and pancreatic cancer cell lines. BSA01 inhibited tumor growth in vivo in multiple cell-derived xenograft (CDX) and patient-derived xenograft (PDX) models, with enhanced efficacy compared to parental monoclonal or monovalent ADCs and superior activity to reference ADCs in certain models. These results suggest that BSA01 is a robust preclinical candidate for EGFR and MUC1 double positive tumors.


1. Mahanta, S., Fessler, S. P., Park, J., & Bamdad, C. (2008). A minimal fragment of MUC1 mediates growth of cancer cells. PloS one, 3(4), e2054. https://doi.org/10.1371/journal.pone.0002054


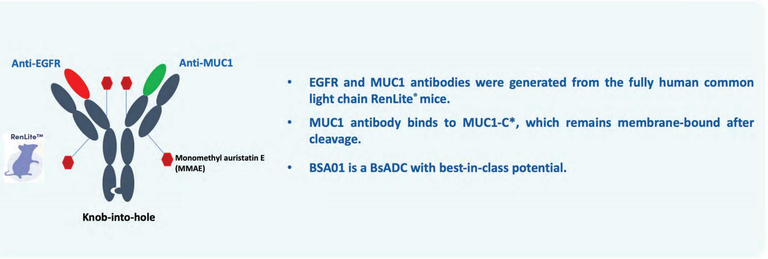


- EGFR and MUC1 antibodies were generated from the fully human common light chain RenLite® mice.
- MUC1 antibody binds to MUC1-C*, which remains membrane-bound after cleavage.
- BSA01 is a BsADC with best-in-class potential.

## Identification of an antibody targeting cleaved, membrane bound MUC1-C*

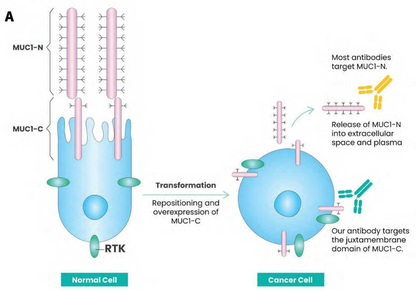


**A. Diagram of MUC1 processing during cell transformation (adapted from DW.Kufe[1]). MUC1-N is shed from the surface of cancer cells.** As a result, the free MUC1-N domain may sequester anti-MUC1 antibodies in circulation and reduce the fraction of antibodies that bind MUC1 proteins on the cell surface after cleavage. The targeting of the juxtamembrane ectodomain of MUC1 may be a better strategy to improve efficacy.

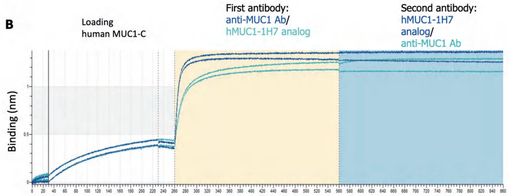


**B. Anti-MUC1 Ab shares epitope on MUC1-C* with a reference anti-MUC1 antibody clone 1H7.** 1H7 clone recognizes MUC1-C*, which is the membrane-bound MUC1 after cleavage[2]. In this binding competition assay, sequential injection of anti-MUC1 Ab followed by 1H7 induced no additional binding signal (ForteBio Octet), and vise versa, indicating anti-MUC1 Ab and 1H7 target overlapping epitopes on MUC1-C*.


1. Kufe, D. MUC1-C oncoprotein as a target in breast cancer: activation of signaling pathways and therapeutic approaches. Oncogene 32, 1073–1081 (2013). https://doi.org/10.1038/onc.2012.158
2. Wu, G., Kim, D., Kim, J. N., Park, S., Maharjan, S., Koh, H., Moon, K., Lee, Y., & Kwon, H. J. (2018). A Mucin1 C-terminal Subunit-directed Monoclonal Antibody Targets Overexpressed Mucin1 in Breast Cancer. Theranostics, 8(1), 78–91. https://doi.org/10.7150/thno.21278


## Identification of an antibody targeting cleaved, membrane bound MUC1-C* (cont'd)

**C. Species cross-reactivity of MUC1 antibodies (FACS).** Anti-MUC1Ab binds both human and cynomolgus monkey exogenously expressed MUC1. **D.** Affinity measurement (Biacore). Anti-MUC1 Ab showed similar affinity to human and cynomolgus monkey antigens. E. IHC staining of patient-derived xenograft models (PDXs) showing cell membrane expression of MUC1 (anti-MUC1 Ab).

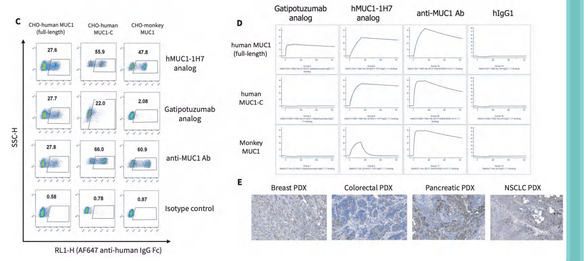


## BSA01 (unconjugated) showed strong binding avidity to EGFR⁺MUC-1⁺ cells but not EGFR⁺MUC-1$^{neg}$ cells

**Cell surface binding of anti-EGFR and anti-MUC-1 antibodies (bispecific, monoclonal and monovalent) were determined by flow cytometry.** Notably, BSA01 (unconjugated) bound double positive HCC827 and HCC70 cells more readily than the single positive A431 cells, with approximately an 8-fold difference in EC50 values. Anti-EGFR (MUC1) Ab or ADC in this poster denotes the parental bivalent (mAb) or monovalent (as indicated) antibodies or ADC, respectively.

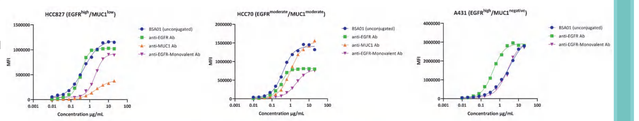


| | Tumor cells | | | | | |
|---|---|---|---|---|---|---|
| | HCC827 ( NSCLC ) | | HCC70 (Triple negative breast cancers ) | | A431 ( Epidermal cancer ) | |
| | EC50 (μg/mL) | maximum binding (MFI) | EC50 (μg/mL) | maximum binding (MFI) | EC50 (μg/mL) | maximum binding (MFI) |
| BSA01 (unconjugated) | 0.5 | 1160000 | 0.4 | 1460000 | 3.3 | 2800000 |
| anti-EGFR Ab | 0.3 | 1030000 | 0.3 | 811000 | 0.4 | 2960000 |
| anti-MUC1 Ab | 2.2 | 377516 | 1.1 | 1560000 | - | - |
| anti-EGFR-Monovalent Ab | 1.9 | 906000 | 2.0 | 756000 | 2.7 | 2840000 |

## BSA01 (unconjugated) demonstrated enhanced internalization compared with monovalent parental antibodies

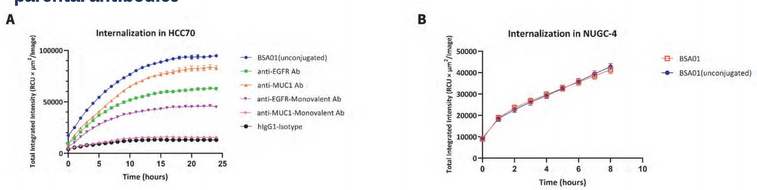


**Internalization of BSA01 and parental antibodies as measured by Incucyte® live-cell assays.**
**A.** BSA01 (unconjugated) demonstrated enhanced internalization compared with monovalent parental antibodies in HCC70 (EGFR$^{moderate}$/MUC1$^{moderate}$).
**B.** BSA01 and BSA01 (unconjugated) exhibited nearly identical internalization activity in NUGC-4 (EGFR$^{moderate}$/MUC1$^{moderate}$) cells.

## *In vitro* cytotoxicity of BSA01

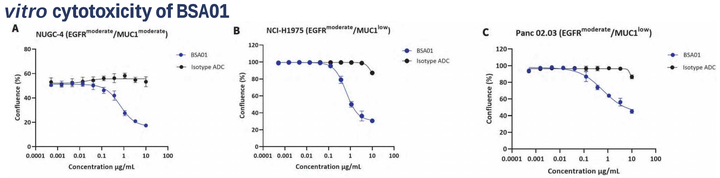


| IC50 (μg/mL) | Tumor cells | | |
|---|---|---|---|
| | NUGC-4 (Gastric cancer) | NCI-H1975 (NSCLC ) | Panc 02.03 (Pancreatic cancer) |
| BSA01 | 0.68 | 0.63 | 0.62 |

**A-C.** BSA01 showed effective killing of NUGC-4 (EGFR$^{moderate}$/MUC1$^{moderate}$), NCI-H1975 (EGFR$^{moderate}$/MUC1$^{low}$) and Panc 02.03 (EGFR$^{moderate}$/MUC1$^{low}$) cells *in vitro*.

## Robust anti-tumor activity of BSA01 in CDX models

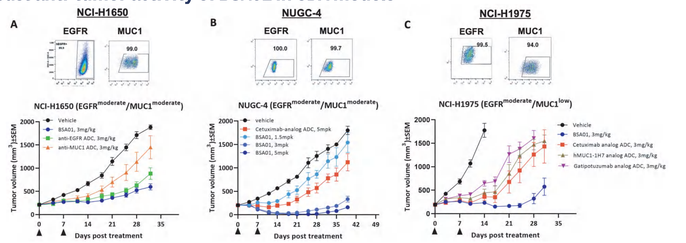


**A.** Increased efficacy of BSA01 in NCI-H1650 xenograft model compared with parental anti-EGFR and anti-MUC1 ADCs. **B.** BSA01 dose-dependently inhibited NUGC-4 xenograft growth. **C.** BSA01 demonstrated stronger antitumor efficacy compared with benchmark ADCs with the same payload/DAR in NCI-H1975 (EGFR L858R & T790M) models.

## Co-expression of EGFR and MUC1 in PDX models

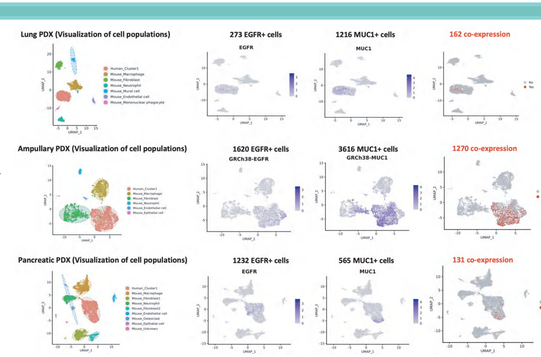


10x Genomic single-cell RNA sequencing of patient-derived xenograft (PDX) models indicates co-expression of EGFR and MUC1 in a subset of cancer cells.

## Potent antitumor efficacy of BSA01 in PDX models

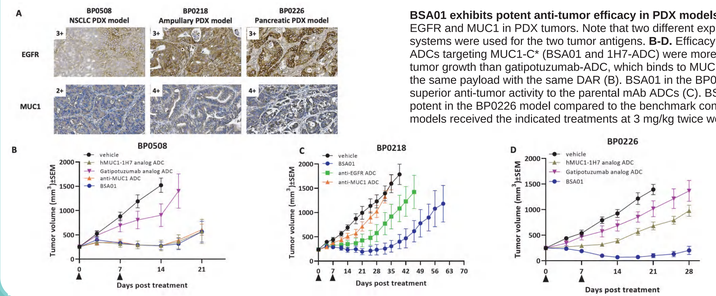


**BSA01 exhibits potent anti-tumor efficacy in PDX models. A.** Expression of EGFR and MUC1 in PDX tumors. Note that two different expression scoring systems were used for the two tumor antigens. **B-D.** Efficacy studies of BSA01. ADCs targeting MUC1-C* (BSA01 and 1H7-ADC) were more potent in inhibiting tumor growth than gatipotuzumab-ADC, which binds to MUC1-N. All ADCs carried the same payload with the same DAR (B). BSA01 in the BP0218 model showed superior anti-tumor activity to the parental mAb ADCs (C). BSA01 was most potent in the BP0226 model compared to the benchmark control ADCs (D). All models received the indicated treatments at 3 mg/kg twice weekly, iv.

## SUMMARY

- Co-expression of EGFR and MUC1 in multiple solid tumors suggests that simultaneous targeting of EGFR and MUC1 with bsADC has the potential to enhance efficacy and improve safety.
- BSA01 is an EGFR- and MUC-1-targeting bsADC derived from the proprietary, RenLite® common light chain, fully human antibody mouse platform.
- BSA01 binds to MUC1-C* that remains membrane bound after cleavage, and exhibits excellent affinity and internalization activity.
- The EGFR arm of BSA01 was selected to have reduced binding and internalization capability, in order to reduce the known skin toxicity of EGFR targeting.
- BSA01 demonstrated potent anti-tumor activity in multiple CDX and PDX models, with improved efficacy over parental mAb ADCs and benchmark ADCs in certain models.

LB212

# BCG022: A novel bispecific antibody-drug conjugate targeting HER3 and MET

Zhuolin Li[1], Chengzhang Shang[1] Xuewa Guan[2], Zhenyan Han[1], Gao An[1], Ellen Zhang[1], Qingcong Lin[1], Yi Yang[1]

[1]Biocytogen Pharmaceuticals (Beijing) Co., Ltd., Beijing, China; [2]Doma Pharmaceutical (Suzhou) Co., Ltd., Suzhou, China

biocytogen.com | info@biocytogen.com

## ABSTRACT

HER3 is a unique EGFR family member that plays a role in both tumor progression and drug resistance. Its expression can act as a bypass mechanism for EGFR and HER2-targeted therapies, resulting in therapeutic resistance. MET has also been reported as a bypass resistance mechanism to EGFR-TKI treatment. HER3 and MET are co-expressed at high prevalence in multiple tumor types, including gastric, colorectal, breast, and non-small-cell lung cancer (NSCLC). In addition, HER3 and MET are frequently overexpressed in liver metastases from patients with colorectal cancer, indicating that targeting both proteins may provide clinical benefit.

We generated fully human bispecific antibodies (bsAbs) targeting HER3 and MET with cross-species reactivity, using RenLite® mice, which contain the full human heavy chain variable domain with a common human kappa light chain to facilitate downstream bispecific antibody assembly. These 1+1 structured bsAbs have demonstrated enhanced internalization compared to the parental monoclonal antibodies in multiple cancer cell lines. These bsAbs were then conjugated with Monomethyl auristatin E (MMAE) to generate HER3 and MET-targeting bispecific ADC (BCG022) candidates.

In vivo drug efficacies are being screened using cell-derived hepatocellular carcinoma (HCC) and gastric carcinoma xenografts, as well as patient-derived gastric and pancreatic xenograft models. Collectively, these results suggest that BCG022 has the potential to be a novel therapeutic option for HER3 and MET co-expressing tumors.

## Co-expression of HER3 and MET in multiple tumor subtypes

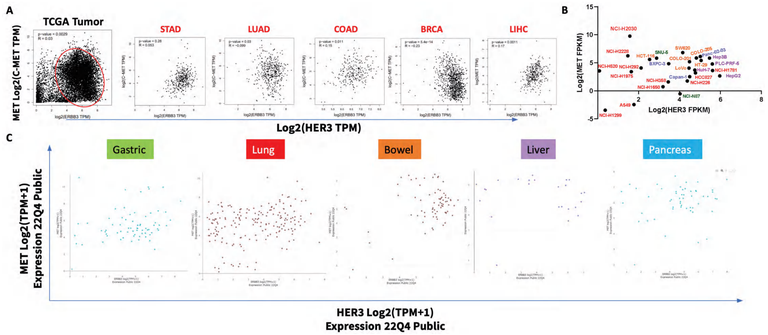


A. Correlative analysis of expression data from multiple cancer types and tissues revealed expression of HER3 (ERBB3) and MET in multiple tumors, especially in potentiated lung adenocarcinoma (LUAD), stomach adenocarcinoma (STAD), colorectal adenocarcinoma (COAD), breast cancer (BRCA) and liver hepatocellular carcinoma (LIHC). Data from the GEPIA 2 database[1]. TCGA, Cancer Genome Atlas. B-C. RNA-Seq results (in-house analyses (B) and Depmap public expression database[2] (C)) indicate that HER3 and MET are co-expressed in a variety of tumor lines, including lung (red), gastric (green), liver (purple), colorectal (orange) and pancreatic (blue) cancers.

[1]Tang Z, Kang B, Li C, Chen T, Zhang Z. GEPIA2: an enhanced web server for large-scale expression profiling and interactive analysis. Nucleic Acids Res. 2019 Jul 2;47(W1):W556-W560. doi: 10.1093/nar/gkz430.
[2]Cancer Dependency Map, 22Q4 release (www.depmap.org/portal)

## BCG022 binding to multiple tumor cell lines

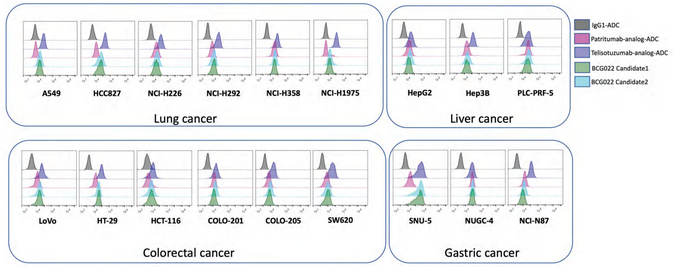


Evaluation of BCG022 binding to multiple lung, liver, colorectal and gastric cancer cell lines with various expression levels of HER3 and MET. BCG022 binds to multiple tumor cell lines with high avidity.

## BCG022 BsAbs demonstrated enhanced internalization compared to parental antibodies

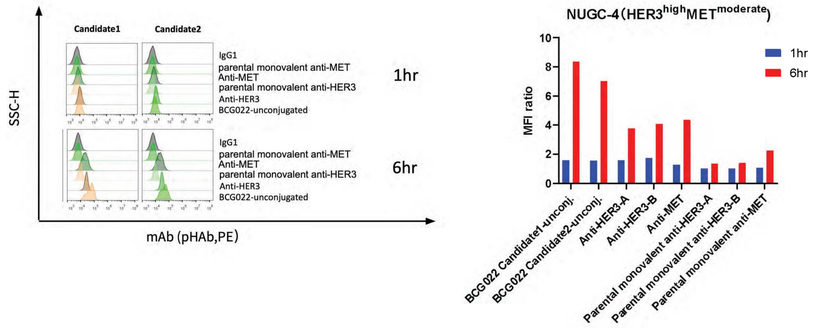


Unconjugated BCG022 candidates showed increased endocytosis activity compared with parental antibodies (anti-MET and anti-HER3) in tumor cells co-expressing HER3/MET (NUGC-4 cells). Furthermore, the internalization induced by parental monovalent anti-HER3 or parental anti-MET was further reduced, indicating that the internalization of monovalent BCG022 targeting HER3 and MET were both modulated.

## *In vitro* cell killing activity of BCG022 candidates

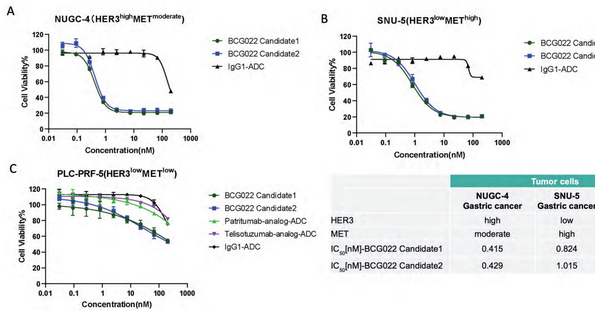


A-B. BCG022 can effectively kill NUGC-4 (HER3$^{high}$ MET$^{moderate}$) and SNU-5 (HER3$^{low}$ MET$^{high}$) gastric cancer cells *in vitro*.

C. BCG022 exhibits stronger killing activity in the PLC-PRF-5 line compared to the benchmark ADCs.

| | Tumor cells | | |
|---|---|---|---|
| | NUGC-4 Gastric cancer | SNU-5 Gastric cancer | PLC-PRF-5 Liver cancer |
| HER3 | high | low | low |
| MET | moderate | high | low |
| $IC_{50}$[nM]-BCG022 Candidate1 | 0.415 | 0.824 | NA |
| $IC_{50}$[nM]-BCG022 Candidate2 | 0.429 | 1.015 | NA |

## Antitumor activity of BCG022 in CDX

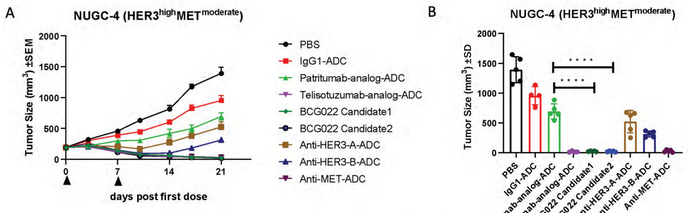


5 × 10$^6$ NUGC-4 cells were injected subcutaneously into in B-NDG mice. When the tumors reached 200 mm$^3$, the mice were randomly grouped (day 0) and treated with PBS or ADCs at both day 0 and day 7.
A. Inhibition of tumor growth induced by BCG022 candidates (i.v., 3 mg/kg, Q2W) was stronger than the anti-HER3 benchmark antibody ADC (Patritumab-analog ADC) and was comparable to the MET benchmark ADC (Telisotuzumab-analog ADC). B. Tumor size at the endpoint. Significance was determined by one-way ANOVA followed by Tukey's multiple comparison test. Error bars indicate SD. ****P < 0.0001.

## Antitumor activity of BCG022 in PDX

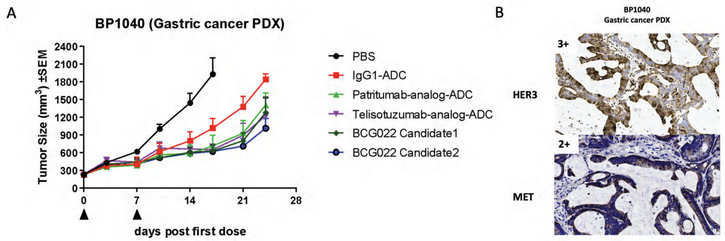


A. Inhibition of BP1040 (gastric cancer PDX) tumor growth in B-NDG mice. Mice were treated with 3 mg/kg (i.v.; Q2W). BCG022 candidate 2 exhibited stronger anti-tumor activity than benchmark ADCs, while BCG022 candidate 1 performed similar to benchmarks. B. Immunohistochemistry staining of HER3 and MET in the PDX tumors. Results indicate moderate levels of MET (2+) and strong staining of HER3 (3+). Error bars indicate SEM.

## BCG022 is a first-in-class bispecific HER3 x MET ADC with human and monkey cross-reactivity

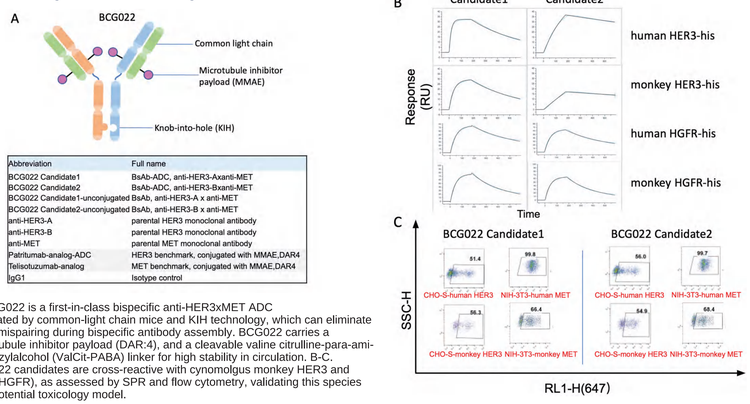


| Abbreviation | Full name |
|---|---|
| BCG022 Candidate1 | BsAb-ADC, anti-HER3-Axanti-MET |
| BCG022 Candidate2 | BsAb-ADC, anti-HER3-Bxanti-MET |
| BCG022 Candidate1-unconjugated | BsAb, anti-HER3-A x anti-MET |
| BCG022 Candidate2-unconjugated | BsAb, anti-HER3-B x anti-MET |
| anti-HER3-A | parental HER3 monoclonal antibody |
| anti-HER3-B | parental HER3 monoclonal antibody |
| anti-MET | parental MET monoclonal antibody |
| Patritumab-analog-ADC | HER3 benchmark, conjugated with MMAE,DAR4 |
| Telisotuzumab-analog | MET benchmark, conjugated with MMAE,DAR4 |
| IgG1 | Isotype control |

A. BCG022 is a first-in-class bispecific anti-HER3xMET ADC generated by common-light chain mice and KIH technology, which can eliminate chain mispairing during bispecific antibody assembly. BCG022 carries a microtubule inhibitor payload (DAR:4), and a cleavable valine citrulline-para-aminobenzylalcohol (ValCit-PABA) linker for high stability in circulation. B-C. BCG022 candidates are cross-reactive with cynomolgus monkey HER3 and MET (HGFR), as assessed by SPR and flow cytometry, validating this species as a potential toxicology model.

## BCG022 induces stronger endocytosis than parental HER3-ADCs in a HER3 $^{low}$ cell line

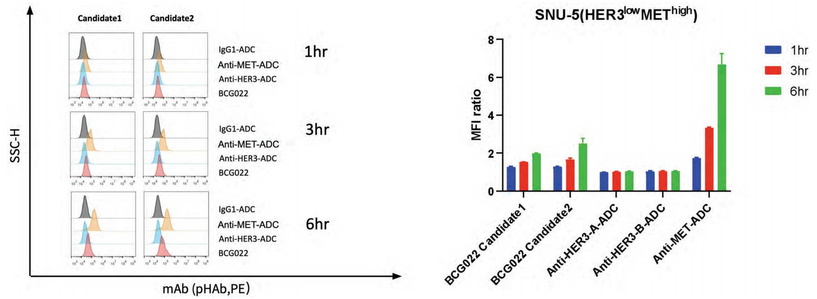


Internalization assessment in SNU-5 (HER3$^{low}$/MET$^{high}$) cells indicates that the endocytosis activity of BCG022 candidates is stronger than that of the parental HER3 monoclonal ADC in a HER3$^{low}$ cancer cell line model. Error bars indicate SD.

## SUMMARY

- **BCG022 is a novel and fully human bispecific antibody-drug conjugate generated from the RenLite® platform that exhibits cross-species reactivity to human and cynomolgus monkey HER3 and MET.**
- **BCG022 candidates can bind a wide range of HER3/MET co-expressing cancer cell lines, including NSCLC, gastric, liver, colorectal and pancreatic cancers.**
- **BCG022 demonstrated higher endocytosis in HER3/MET co-expressing tumor cells than parental HER3 monoclonal ADCs, and stronger tumor growth inhibition than parental ADCs.**
- **BCG022 showed strong anti-tumor efficacy in both CDX and PDX models.**

LB216

# Discovery of BCG033, a novel anti-PTK7 x TROP2 bispecific antibody-drug conjugate with promising efficacy against triple-negative breast cancer

Sufei Yao, Chengzhang Shang, Gao An, Ellen Zhang, Qingcong Lin, Yi Yang

Biocytogen Pharmaceuticals (Beijing) Co., Ltd., Beijing, China

biocytogen.com | info@biocytogen.com

## ABSTRACT

Triple-negative breast cancer (TNBC) accounts for 15-20% of metastatic breast cancer incidence, and remains an area of unmet clinical need due to the low rates of overall survival. Recently, the TROP2-targeting ADC sacituzumab govitecan has received an accelerated approval from the FDA for adult patients with metastatic TNBC, as more than 85% of TNBC is marked by TROP2 overexpression. However, the clinical efficacy of ADC therapies targeting TROP2 alone is limited by its on-target toxicity. In an effort to offer therapeutic alternatives that limit this toxicity, we sought to identify other targets to combat metastatic TNBC in combination with TROP2. PTK7 is highly expressed in breast cancer; notably, PTK7 expression is higher in TNBC than non-TNBC, and is correlated with worse prognosis, tumor metastasis and TNBC progression. PTK7 has also been demonstrated to be enriched in tumor-initiating cells (TICs) in low-passage TNBC, OVCA, and NSCLC patient derived xenografts (PDXs). We generated fully human anti-human PTK7 x TROP2 bispecific antibodies (bsAbs) from RenLite® mice, which harbor the complete human heavy chain immunoglobulin variable domain with a common human kappa light chain for subsequent bispecific antibody assembly. These bsAbs demonstrated reactivity to human, monkey, and dog antigens, and showed enhanced internalization in vitro compared with parental PTK7 antibodies. In addition, these bsAbs showed favorable tumor cell selectivity, as there was minimal internalization of the monovalent antibodies. These bsAbs were then conjugated with Monomethyl auristatin E (MMAE) to generate anti-PTK7 x TROP2 bispecific ADC (BCG033) candidates. BCG033 candidates showed potent anti-tumor activity in several cell line derived xenografts including TNBC xenografts, indicating that BCG033 has strong therapeutic potential in TNBC and other PTK7/TROP2 co-expressing cancers. Patient-derived TNBC xenografts with co-expression of PTK7 and TROP2 have been screened for future in vivo drug efficacy screening. In summary, BCG033 has the potential to exert anti-tumor efficacy in TNBC and other solid tumors co-expressing PTK7 and TROP2.

## Strong binding activity of anti-PTK7/TROP2 BsAbs

Binding of unconjugated BCG033 candidates to several cell lines was assessed by flow cytometry. BCG033 candidates (blue, green) showed strong binding activity to a variety of TNBC cell lines, as well as to other tumor types.

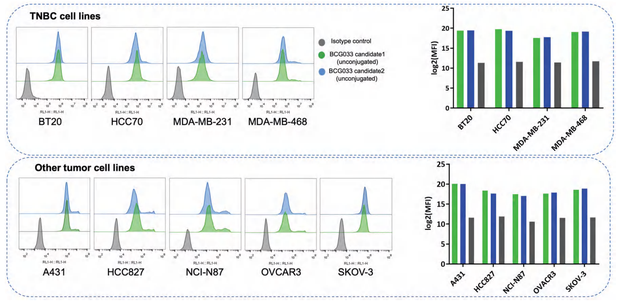


## Antitumor activity of BCG033 candidates *in vivo*

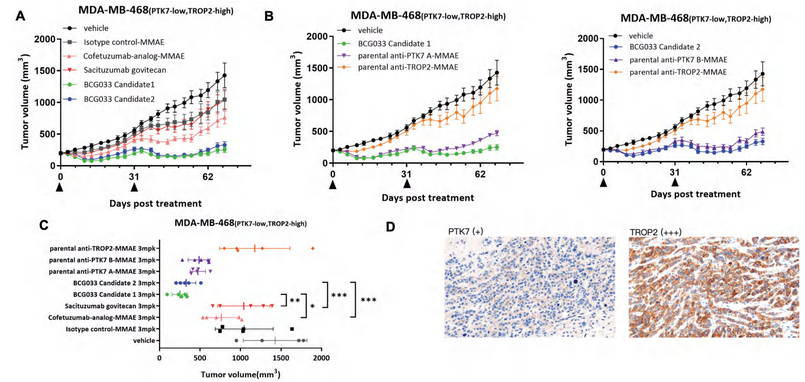


1 × $10^7$ MDA-MB-468 cells were injected subcutaneously into each B-NDG (immunodeficient) mouse. When the tumors reached 200 $mm^3$, the mice were randomly grouped and injected with the 1st dose of phosphate buffer saline (PBS) or ADCs (3 mpk) by intravenous (i.v.) administration (day 0). The second dose was given on day 31. BCG033 candidates showed robust anti-tumor efficacy in cell line-derived TNBC xenografts (MDA-MB-468, $PTK7^{low}/TROP2^{high}$), which was more pronounced than that induced by benchmark ADCs (A) and parental Ab-ADCs (B). Data from A-C is from one experiment parsed into different graphs to compare the potency of different test articles within that experiment. (C) Comparison of all conditions from A-B at the final endpoints. Significance was determined by one-way ANOVA followed by Tukey's multiple comparison test. Error bars indicate SD. *P ≤ 0.05, * * P ≤ 0.01 ***P < 0.001. (D) Immunohistochemical analysis of PTK7 and TROP2 in MDA-MB-468 tumors *in vivo*.

## Co-expression of PTK7/TROP2 in multiple cancer cell types

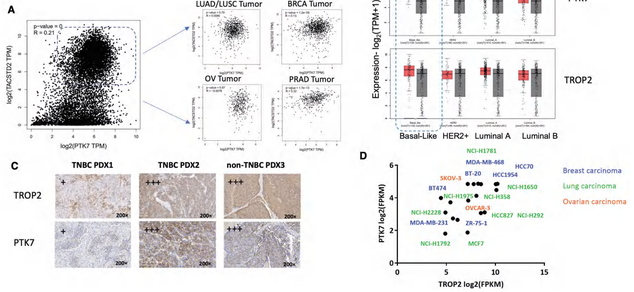


A, B. Expression data from the GEPIA2 database[1] indicates that PTK7 is co-expressed with TROP2 in multiple tumors, especially in lung adenocarcinoma (LUAD), lung squamous cell carcinoma (LUSC), breast cancer (BRCA), ovarian cancer (OV) and prostate adenocarcinoma (PRAD). PTK7 and TROP2 are widely overexpressed in breast cancer, especially in triple-negative tumors. C. IHC staining of internal PDX showed that PTK7 and TROP2 were co-expressed in several models, including TNBC. D. RNA-seq data (in-house analysis) indicates PTK7 and TROP2 were co-expressed in many tumor cell lines, especially in breast, lung and ovarian tumors.

[1]Reference: Tang Z, Kang B, Li C, Chen T, Zhang Z. GEPIA2: an enhanced web server for large-scale expression profiling and interactive analysis. Nucleic Acids Res. 2019 Jul 2;47(W1):W556-W560. doi: 10.1093/nar/gkz430. PMID: 31114875; PMCID: PMC6602440.

## Internalization of anti-PTK7/TROP2 BsAbs

Anti-PTK7/TROP2 bispecific antibodies (BsAb) (2.5 μg/mL) and pHAb-Goat Anti-Human IgG Secondary Antibody were added to BT-20 and HCC70 cells. After incubating for 1,3, and 5 hours, the cells were centrifuged and washed in FACS buffer. MFI of the pH-sensitive dye was detected on a flow cytometer. The anti-PTK7/TROP2 BsAbs showed increased endocytosis activity compared with its parental anti-PTK7 monoclonal antibodies in tumor cells co-expressing PTK7/TROP2, whereas the monovalent anti-TROP2/control or anti-PTK7/control BsAbs showed reduced internalization.

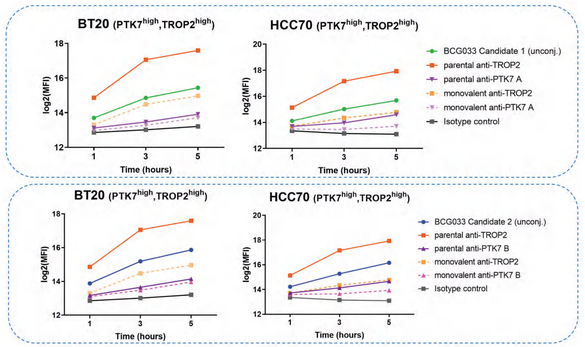


## BCG033 candidates demonstrate potent anti-tumor activity in a breast cancer PDX model

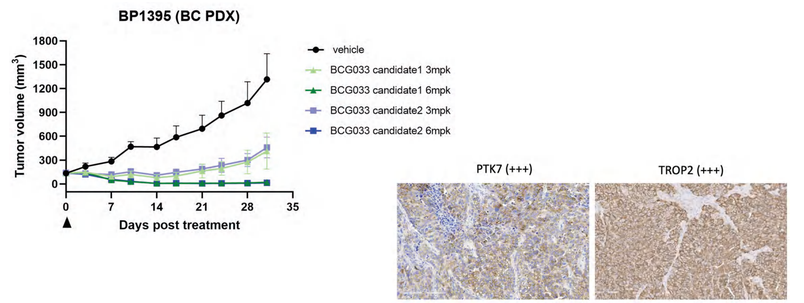


BP1395 (HER2-positive breast cancer) PDX tumor fragments were subcutaneously inoculated into specific pathogen-free female B-NDG immunodeficient mice. When the tumors reached a volume of approximately 140 $mm^3$, the tumor-bearing mice were randomized into treatment and control groups based on tumor volume and dosing was administered on day 0 (arrow). BCG033 candidates showed potent anti-tumor activity in the BC PDX model and induced tumor regression at a single dose of 6 mg/kg. The expression of PTK7 and TROP2 on the BP1395 PDX sample was analyzed by IHC staining as shown.

## BCG033 conjugation and cross-reactivity to human and cynomolgus monkey antigen

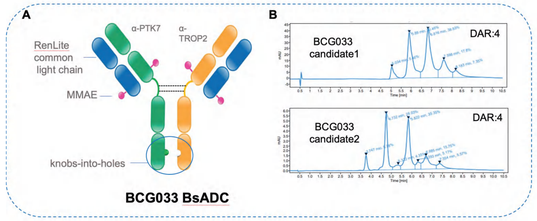


A. We generated fully human anti-human PTK7 x TROP2 bispecific antibodies (bsAbs) from RenLite® mice, which harbor the complete human heavy chain immunoglobulin variable domain with a common human kappa light chain for subsequent bispecific antibody assembly. Using the vedotin ADC technology that delivers the powerful MMAE cytotoxin, BCG033 is a novel bispecific ADC that targets both PTK7 and TROP2. B. Analysis of drug-to-antibody ratio (DAR) by hydrophobic interaction chromatography (HIC). C. BCG033 candidates (unconjugated) demonstrated reactivity to human and cynomolgus monkey antigens, as assessed by flow cytometry.

## *In vitro* cell growth inhibitory activity of BCG033

Purified ADCs with different concentrations (10ug/mL, 3.33ug/mL, 1.11/mL, 0.37ug/mL, 0.12ug/mL, 0.04ug/mL, 0.013ug/mL, 0.004ug/mL , 0.001ug/mL , 0.0005ug/mL) were used to treat HCC70 cells or MDA-MB-468 cells in culture. Killing activity was detected after 72 hours of incubation with IncuCyte® S3 (Sartorius AG).
A. BCG033 candidates showed strong killing activity in HCC70 and MDA-MB-468 cells.
B. The monovalent anti-TROP2-MMAE showed reduced killing activity, suggesting that BCG033 candidates increase the tumor selectivity of payload delivery.

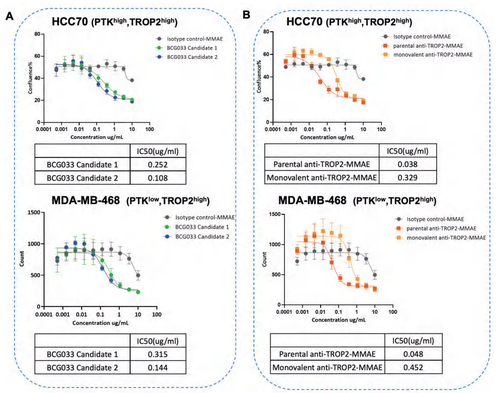


## SUMMARY

- BCG033 is a novel and fully human bispecific PTK7 and TROP2 antibody-drug conjugate generated from the RenLite® platform.
- Cytotoxicity assays and internalization assays indicate a potentially better tumor cell selectivity of BCG003 compared to the parental anti-TROP2 monoclonal. BCG003 induced potent cell killing of PTK7/TROP2 co-expressing tumor cells.
- BCG033 candidates showed potent anti-tumor activity in both TNBC CDX and BC PDX models, indicating that BCG033 has strong therapeutic potential in TNBC and other PTK7/TROP2 co-expressing cancers.
- PTK7/TROP2 is co-expressed in a variety of solid tumors, suggesting multiple potential indications for BCG033.

LB215

# A first-in-class anti-TROP2/EGFR bispecific antibody-drug conjugate, DM001, exhibits potent anti-tumor efficacy

Zhuolin Li[1], Chengzhang Shang[1], Xuewa Guan[2], Gao An[1], Yuming Guo[1], Ellen Zhang[1], Qingcong Lin[1], Yi Yang[1]

[1]Biocytogen Pharmaceuticals (Beijing) Co., Ltd.,Beijing, China; [2]Doma Pharmaceutical (Suzhou) Co., Ltd., Suzhou, China

BIOCYTOGEN

biocytogen.com | info@biocytogen.com

## ABSTRACT

EGFR is a well-established target for the treatment of many cancers. However, limitations encountered with current therapies, such as drug resistance and low cytotoxicity, indicate a need for alternative treatments. Antibody-drug conjugates (ADCs) are a promising new therapeutic strategy, because of their potent killing effects and high target specificity. However, the toxicity of the ADC payload can often cause safety concerns, so their efficacy and safety must be carefully evaluated. With these challenges in mind, we developed a bispecific ADC (BsADC) targeting EGFR and a second tumor-associated antigen with the goal to improve tumor specificity, thereby limiting the occurrence of on-target off-tumor effects. TROP2 and EGFR are co-expressed in multiple types of solid tumors, including head and neck, esophageal, lung, and pancreatic cancers, suggesting that this target combination could provide therapeutic benefit for a wide range of tumors.

Herein, we developed a novel BsADC, DM001, targeting TROP2 and EGFR, conjugated with monomethyl auristatin E (MMAE) via a protease-cleavable linker. *In vitro*, DM001 showed similar levels of internalization and tumor killing activity compared with its parental monoclonal anti-TROP2 and anti-EGFR antibodies in TROP2$^{+}$ EGFR$^{+}$ cells. Compared with single positive cells, DM001 can selectively bind and better kill double positive cells. Mechanistically, DM001 delays progression of the cell cycle and increases the frequency of apoptosis *in vitro* in an antigen-dependent manner. Pharmacokinetic analyses in mice with humanized FcRn (B-hFcRn) demonstrated a similar half-life of DM001 to isotype controls. Importantly, DM001 demonstrated strong anti-tumor activity in several cell line-derived and patient-derived xenografts, including lung and pancreatic tumors. Notably, the efficacy of DM001 was superior to benchmark ADCs in A431 and Panc.02.03 xenografts. Interestingly, the efficacy of DM001 was superior to its parental ADCs in BP0508 lung cancer and BP0209 pancreatic cancer PDX models, but not obvious in Panc.02.03 CDX models, indicating that DM001 may effectively target heterogeneous tumors, which better mimic the tumor microenvironment in patients. In summary, DM001 is a novel bispecific ADC with promising therapeutic potential that can be further exploited to treat TROP2 and EGFR co-expressing tumors.

## Co-expression of TROP2 and EGFR in PDXs

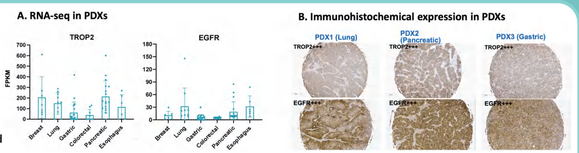


**TROP2 and EGFR are highly co-expressed in patient-derived xenografts (PDX).**
**(A)** RNA-seq data from several PDXs (in-house) were analyzed for expression of TROP2 and EGFR. Both were highly expressed in lung, pancreatic and esophagus cancer tissues.
**(B)** TROP2 and EGFR were also co-expressed in some of PDX samples as assessed by IHC.
**(C)** Co-expression of TROP2 and EGFR in populations identified by single cell (scRNAseq) was also observed in these PDX samples.

## DM001 bsAb showed high affinity and internalization activity

**Binding and internalization activity of DM001 BsAb. (A)** Continuous binding on hTROP2 and hEGFR antigens of DM001 via SPR. **(B)** DM001 affinity measurements by flow cytometry. Expression of TROP2 and EGFR in the cell lines are as follows:
TROP2$^{high}$ EGFR$^{high}$: NCI-H292, Panc.02.03 and BxPC-3;
TROP2$^{high}$ EGFR$^{low}$: NCI-N87;
TROP2$^{low}$ EGFR$^{low}$: NUGC-4 and HELA;
TROP2$^{neg}$ EGFR$^{+}$: NCI-H226;
TROP2$^{neg}$ EGFR$^{neg}$: NCI-H520.
**(C)** Internalization of DM001 BsAb in NCI-H292 and BxPC-3 cells measured by Incucyte.

**Results:** DM001 showed high affinity and increased internalization in several cancer cell lines compared with its parental TROP2 or EGFR monovalent antibodies.

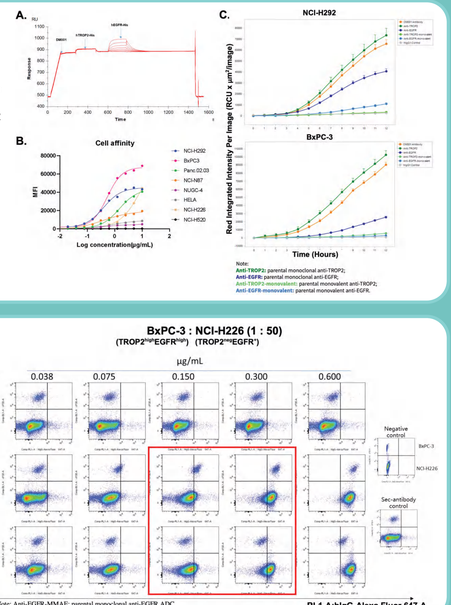


## Selectivity of DM001 bsADC for TROP2$^{+}$EGFR$^{+}$ cells

**DM001 preferentially binds cells that highly express both TROP2 and EGFR.** BxPC-3 (TROP2$^{high}$EGFR$^{high}$) and NCI-H226 (TROP2$^{neg}$EGFR$^{+}$) cells were co-cultured at a ratio of 1:50, respectively, then treated with DM001 and anti-EGFR-MMAE to assess the binding selectivity.

**Results:** DM001 selectively binds double positive BxPC3 cells at lower concentrations (red box). As the concentration increased, DM001 then began to bind single positive NCI-H226 cells. Anti-EGFR-MMAE was used as control.




## DM001 induces cytotoxicity in TROP2$^{+}$EGFR$^{+}$ cells & bystander killing in TROP2$^{neg}$EGFR$^{neg}$ cells

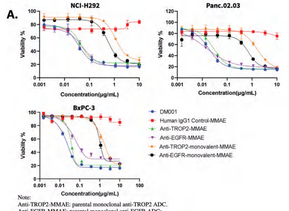


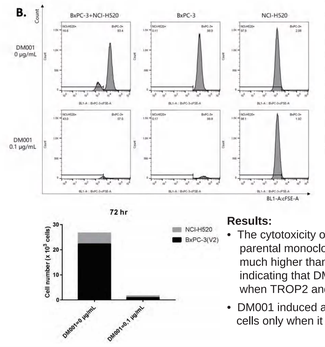


**Cytotoxicity and Bystander effect of DM001 *in vitro*. (A)** Cytotoxicity of DM001 on several cell lines.
**(B)** DM001 induces bystander effects. 0.1 μg/mL DM001 was added to 3 groups: BxPC-3 + NCI-H520, BxPC-3 and NCI-H520. While DM001 induced cytotoxicity of the double positive BxPC-3 cells, double negative NCI-H520 cells were only killed in the presence of BxPC-3 cells. Error bars indicate SD.

**Results:**
- The cytotoxicity of DM001 was comparable to its parental monoclonal TROP2 or EGFR ADCs, and much higher than its parental monovalent ADCs, indicating that DM001 has robust killing activity only when TROP2 and EGFR were both expressed.
- DM001 induced a bystander effect by killing NCI-H520 cells only when it was co-cultured with BxPC-3.

## DM001 delays progression of the cell cycle and induces apoptosis

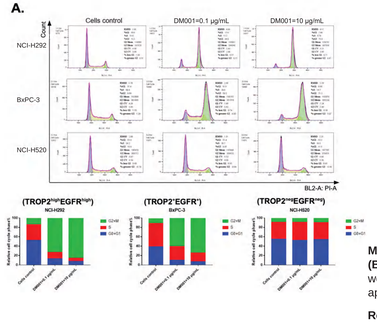


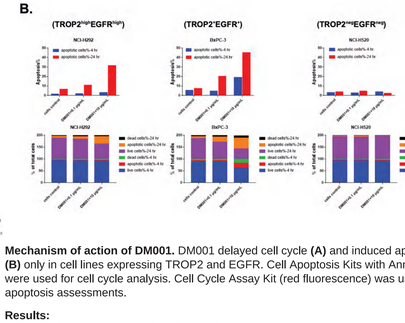


**Mechanism of action of DM001.** DM001 delayed cell cycle **(A)** and induced apoptosis **(B)** only in cell lines expressing TROP2 and EGFR. Cell Apoptosis Kits with Annexin V were used for cell cycle analysis. Cell Cycle Assay Kit (red fluorescence) was used for apoptosis assessments.

**Results:**
DM001 delayed the progression of the cell cycle and increases the frequency of apoptosis *in vitro* in an antigen-dependent manner.

## Pharmacokinetic properties of DM001 in humanized B-hFcRn mice

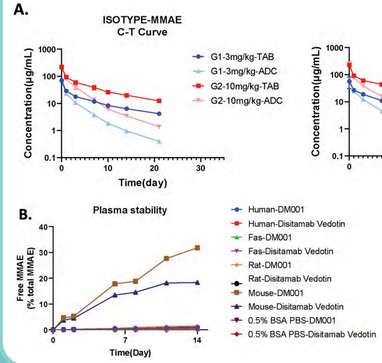


| | | T1/2 (day) | |
|---|---|---|---|
| | | ADC | Tab |
| ISO-MMAE | 3mpk | 5.069 | 11.365 |
| | 10mpk | 5.088 | 10.335 |
| DM001 | 3mpk | 5.053 | 13.318 |
| | 10mpk | 4.818 | 10.581 |

**The concentration of total antibody (TAB) and DM001 ADC in B-hFcRn mice serum. (A)** Serum pharmacokinetic analyses in mice with humanized FcRn (B-hFcRn). TAB, total antibody. Error bars indicate SD. **(B)** Stability of DM001 in plasma of different species.

**Results:**
Pharmacokinetic analyses in mouse serum demonstrated a similar half-life of DM001 to isotype controls. To determine whether the reduction in ADC concentration over time results in increased MMAE release, the percentage of free MMAE was assessed in plasma, which indicates that about 30% of the MMAE was released after 14 days in mice. This may be due to the presence of CES1c in mouse blood.

## DM001 exhibits dose-dependent anti-tumor efficacy in CDX models

**Anti-tumor efficacy of DM001 in CDX. DM001 efficacy was assessed in NCI-H292 (TROP2$^{high}$EGFR$^{high}$) (A) and (B) Panc.02.03 (TROP2$^{high}$EGFR$^{high}$) CDX models.** Tumor samples were analyzed by immunohistochemistry. Different concentrations of DM001 (1mpk, 3mpk, 10mpk) were administered intravenously once a week as indicated (blue arrows). Error bars indicate SEM.

**Results:**
DM001 showed strong and dose-dependent anti-tumor efficacy in NCI-H292 and Panc.02.03 CDX models. At the 10 mpk dose, DM001 completely abolished NCI-H292 tumor growth after Day 14.

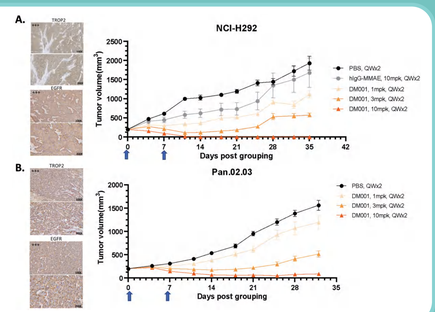


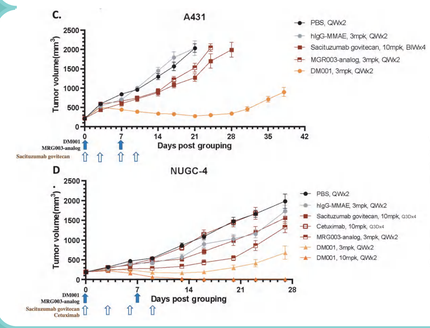


**DM001 efficacy assessments in A431 (TROP2$^{high}$EGFR$^{high}$) (C) and NUGC-4 (TROP2$^{low}$EGFR$^{low}$) (D) CDX models.** DM001 was administered intravenously once a week (2x total) as indicated. Sacituzumab govitecan was intravenously administered twice a week or once per 3 days (4x total) as a benchmark for TROP2 ADC. Cetuximab was intravenously administered twice a week or once per 3 days (4x) as a benchmark for EGFR. MRG003-analog was intravenously dosed once a week (2x total) as a benchmark for EGFR ADC. Error bars

**Results:**
DM001 showed strong and superior anti-tumor efficacy in A431 and NUGC-4 CDX models compared to the benchmarks Sacituzumab govitecan, Cetuximab and MRG003-analog.

## Anti-tumor efficacy of DM001 in PDX models

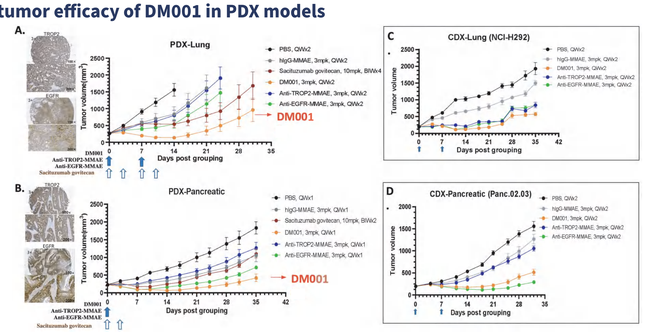


**Anti-tumor efficacy of DM001 in PDX models.** DM001 was assessed in lung (TROP2$^{high}$EGFR$^{high}$) **(A)** and pancreatic (TROP2$^{high}$EGFR$^{high}$) **(B)** PDX models. DM001 was intravenously administered once a week (1x total) at a dosage of 3 mpk. Sacituzumab govitecan (a benchmark of TROP2 ADC) was intravenously administered twice a week (2x total) at a dosage of 10 mpk. **(C-D)** Efficacy of DM001 in lung (TROP2$^{high}$ EGFR$^{high}$) and pancreas (TROP2$^{high}$ EGFR$^{low}$) CDX models was similarly assessed. Error bars indicate SEM.

**Results:** DM001 showed strong anti-tumor efficacy in these two PDX models at a dosage of 3 mpk. The efficacy was more potent than benchmark Sacituzumab govitecan and its parental ADCs.

## SUMMARY

***In vitro* efficacy of DM001**：
DM001 showed high affinity and cytotoxicity in multiple TROP2$^{+}$ EGFR$^{+}$ cancer cell lines.
DM001 delayed cell cycle progression and induced apoptosis in cancer cells.
DM001 bsADC showed preferential binding to cells expressing both TROP2 and EGFR, indicating potentially better safety in single positive cells.

***In vivo* efficacy of DM001**：
DM001 exhibited potent and dose-dependent anti-tumor efficacy in multiple CDX and PDX models. DM001 showed stronger efficacy than benchmarks Sacituzumab govitecan, Cetuximab and MGR003-analog.
While the efficacy of DM001 was higher than its parental ADCs in PDX models, it was not obvious in CDX models, indicating that DM001 may be more effective in targeting heterogeneous tumors, which better mimics the tumor microenvironment in patients.

LB214

# A first-in-class bispecific antibody-drug conjugate (DM002) targeting HER3 and the juxtamembrane domain of MUC1

Yifu Zhang[1], Chengzhang Shang[1], Nannan Wang[2], Gao An[1], Ellen Zhang[1], Qingcong Lin[1], Yi Yang[1]

[1]Biocytogen Pharmaceuticals (Beijing) Co., Ltd., Beijing, China; [2]Doma Pharmaceutical (Suzhou) Co., Ltd., Suzhou, China

biocytogen.com | info@biocytogen.com

## ABSTRACT

Despite the entry of new anti-cancer drugs into the market, there were more than 10 million deaths from cancer globally in 2021[1], with cancers of the lung, stomach, breast, and pancreas contributing to the most cancer-related deaths in China and the USA[2,3]. Accordingly, there is an urgent need for improved therapeutic interventions. Antibody-drug conjugates (ADC) are novel drugs that exploit the specificity of a monoclonal antibody for target antigens expressed on cancer cells in order to achieve targeted delivery of a potent cytotoxic payload. More recently, bispecific ADCs (BsADC) targeting two tumor-associated antigens (TAA) have been developed to further amplify tumor c with other currently available HER3 mAb. These bsAbs were subsequently conjugated with monomethyl auristatin E (MMAE) via a protease-cleavable linker to obtain first-in-class BsADC candidates, DM002. DM002 candidates showed robust anti-tumor activity in multiple CDX and PDX models of lung, breast, gastric and pancreatic cancer; most notably, DM002 candidates outperformed benchmark ADCs in BP0508 lung PDX models. Together, these data indicate that DM002 will be a promising therapeutic drug for patients with HER3 and MUC1 co-expressing tumors.

[1] World Health Organization: "Cancer."
[2] Siegel, RL, Miller, KD, Fuchs, HE, Jemal, A. Cancer statistics, 2022. CA Cancer J Clin. 2022.
[3]Xia C, Dong X, Li H, Cao M, Sun D, He S, Yang F, Yan X, Zhang S, Li N, Chen W. Cancer statistics in China and United States, 2022: profiles, trends, and determinants. Chin Med J (Engl). 2022 Feb 9;135(5):584-590.

## Co-expression of HER3 and MUC1 in tumors

**A)** Correlation analysis indicates that HER3 and MUC1 are commonly co-expressed in multiple tumors, especially in LUAD (lung), BRCA (breast), and PAAD (pancreas), according to the GEPIA 2 database[1]. TCGA, Cancer Genome Atlas.
**B)** Single-cell RNA sequencing results demonstrate HER3 co-expression with MUC1 in some PDX sample cell populations.

[1]Reference: Tang Z, Kang B, Li C, Chen T, Zhang Z. GEPIA2: an enhanced web server for large-scale expression profiling and interactive analysis. Nucleic Acids Res. 2019 Jul 2;47(W1):W556-W560. doi: 10.1093/nar/gkz430.

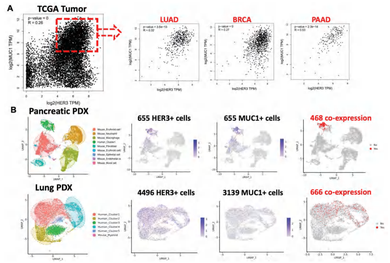


## DM002 candidates demonstrate robust anti-tumor activity in CDX models

**Efficacy of DM002 *in vivo*.** Treatment with test articles indicated by arrows. Each CDX experiment in A and B was parsed into two graphs to compare the potency of each dose and test article. **A)** Both DM002 candidates demonstrate robust anti-tumor activity in cell line-derived xenografts with different levels of HER3 expression, especially HCC70 (HER3$^{low}$MUC-1$^{med}$); efficacy was stronger or comparable to their benchmark ADCs. **B)** DM002 candidates showed superior or comparable anti-tumor activity compared with the parental Ab-ADCs. GC: gastric cancer, BC: breast cancer.

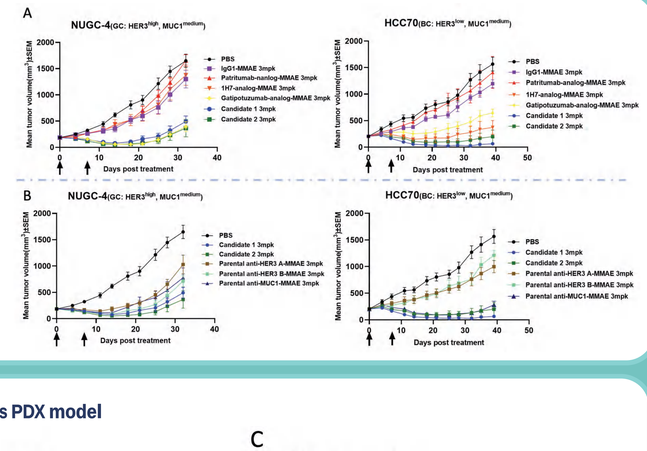


## DM002 exhibits robust anti-tumor activity in the BP0141 pancreas PDX model

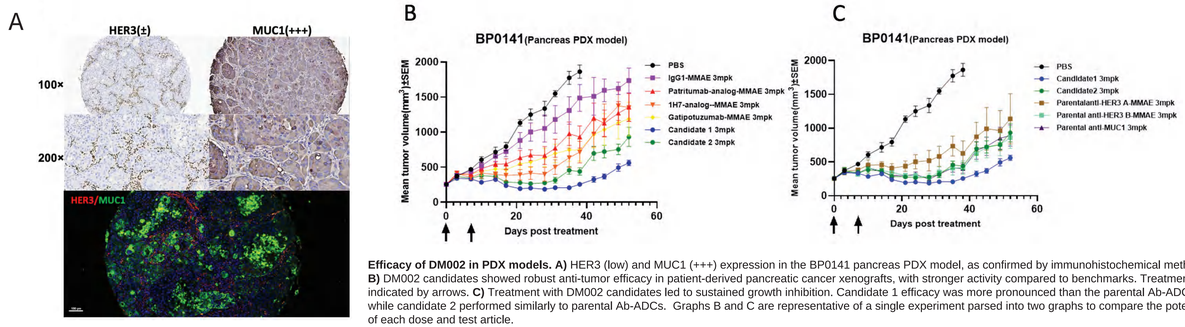


**Efficacy of DM002 in PDX models. A)** HER3 (low) and MUC1 (+++) expression in the BP0141 pancreas PDX model, as confirmed by immunohistochemical methods. **B)** DM002 candidates showed robust anti-tumor efficacy in patient-derived pancreatic cancer xenografts, with stronger activity compared to benchmarks. Treatments indicated by arrows. **C)** Treatment with DM002 candidates led to sustained growth inhibition. Candidate 1 efficacy was more pronounced than the parental Ab-ADCs, while candidate 2 performed similarly to parental Ab-ADCs. Graphs B and C are representative of a single experiment parsed into two graphs to compare the potency of each dose and test article.

## DM002 discovery workflow and characterization

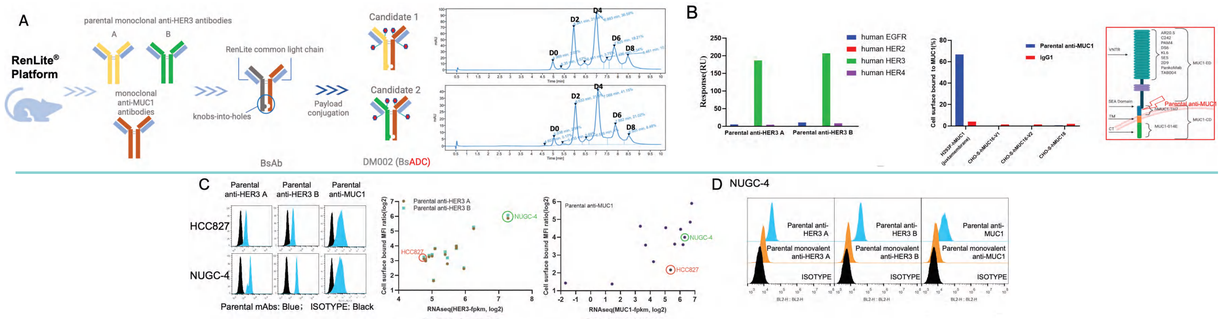


**A)** Two parental anti-HER3 antibodies (A&B) and one parental anti-MUC1 antibody were screened from RenLite® mice, which contain the full human heavy chain variable domain with a common human light chain. Antibodies were then assembled into two DM002 candidates. Both DM002 candidates carry a MMAE payload (DAR ~4) via a cleavable VC-PAB linker. **B)** Parental anti-HER3 antibodies A and B, and parental anti-MUC1 antibody do not recognize other EGFR family members as assessed by SPR. Binding assessments (flow cytometry) indicate that parental anti-MUC1 targets the juxtamembrane domain of MUC1 and prevents antibody neutralization induced by shedding of MUC1-N. Image from Bose et al., 2020. **C)** Parental antibodies can bind to multiple tumor cell lines with different HER3 and MUC1 expression levels as measured by RNA sequencing. **D)** Parental antibodies showed high endocytic activity compared with the parental monovalent antibodies.

Bose, M.; Mukherjee, P. Potential of Anti-MUC1 Antibodies as a Targeted Therapy for Gastrointestinal Cancers. Vaccines 2020, 8, 659. https://doi.org/10.3390/vaccines8040659

## DM002 demonstrates robust anti-tumor activity in the BP0508 lung PDX model

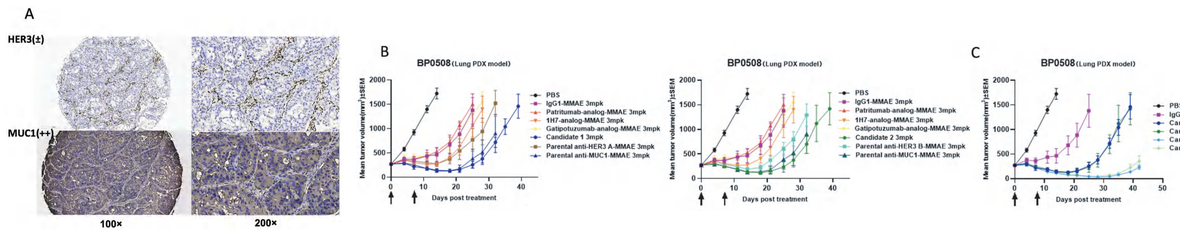


**DM002 efficacy in patient-derived lung cancer xenografts (BP0508) with (A) low expression of HER3 indicated by IHC. B)** Both DM002 candidates showed robust anti-tumor activity stronger than benchmarks and parental HER3 Ab-ADCs. **C)** The anti-tumor activity of DM002 candidates is dose-dependent. Graphs are representative of a single experiment parsed into three graphs to compare the potency of each dose and test article.

## Unconjugated DM002 candidates exhibit cross-species reactivity and induce endocytosis

**A.** The affinity of unconjugated DM002 to both HER3 and the juxtamembrane domain of MUC1 (human and cynomolgus monkey) are about $10^{-8}$ M (KD), measured by SPR. **B, C.** Unconjugated DM002 candidates can bind to cells with different levels of HER3 and showed stronger binding than their parental HER3 antibodies in HER3$^{low}$ tumor cells (HCC827). **D.** The endocytosis activity of DM002 candidates was not altered after conjugation. Internalization of unconjugated DM002 was better than its parental monoclonal antibodies, reflecting a synergistic effect, and was also stronger than the benchmark antibodies.

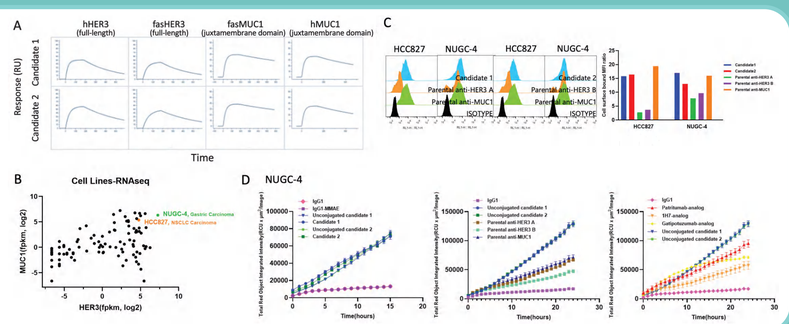


## SUMMARY

- HER3 and MUC1 are co-expressed in a variety of solid tumors, especially those with the highest mortality.
- DM002 is a novel fully human bispecific antibody-drug conjugate generated by the RenLite® common light chain mouse platform. DM002 cross-reacts with human and monkey HER3 and the MUC1 juxtamembrane domain.
- DM002 displayed higher endocytosis activity and more potent tumor growth inhibition of HER3 and MUC1 co-expressing tumors (especially HER3$^{low}$ tumors) compared to HER3 and MUC-1 benchmarks.
- DM002 is a promising first-in-class ADC with potential to treat a variety of HER3 and MUC-1-expressing cancers.

LB213

# Identification of DM004, a first-in-class anti-5T4/MET bispecific antibody-drug conjugate

Zhenyan Han[1], Chengzhang Shang[1], Wenjuan Dai[2], Gao An[1], Ellen Zhang[1], Qingcong Lin[1], Yi Yang[1]

[1]Biocytogen (Pharmaceuticals) Beijing Co., Beijing, China; [2]Doma Biopharmaceutical (Suzhou) Co., Ltd, Suzhou, China

biocytogen.com | info@biocytogen.com

## ABSTRACT

Aberrant MET signaling is frequently found in various types of solid tumors, and correlates to oncogenic transformation, treatment resistance and poor prognosis. While MET remains an attractive therapeutic target, it is widely expressed on the surface of epithelial and endothelial cells, including normal tissues and tumors. To date, MET-targeting agents are associated with adverse clinical effects, including hypoalbuminemia, peripheral edema and pneumonitis, indicating that alternate treatments and/or modalities are needed. Intriguingly, MET antigen is commonly co-expressed with the oncofetal antigen 5T4 in various cancer types, including head and neck, lung and pancreatic cancer. While 5T4 is highly expressed on primary and metastatic cancers and is associated with adverse clinical outcomes in solid tumors, expression on normal adult tissues is very limited. Although several therapeutic agents targeting 5T4 antigen are currently being evaluated in human clinical studies, none have yet entered the market.

To address these challenges, we hypothesized that targeting both MET and 5T4 with a bispecific antibody-drug conjugate (BsADC) could provide a more targeted therapeutic strategy to effectively eliminate tumor cells and reduce systemic toxicity. Here, we report that we have successfully generated two bispecific antibody candidates targeting both 5T4 and MET. The candidates were conjugated with monomethyl auristatin E (MMAE) via a protease-cleavable linker to generate DM004 BsADCs, i.e., Top1-MMAE and Top2-MMAE. In vitro, DM004 BsAbs demonstrated enhanced internalization on the NCI-H226 cell line compared to its parental monoclonal and monovalent anti-5T4 and anti-MET antibodies. In vivo, DM004 BsADCs exhibited robust anti-tumor activity in cell line-derived and patient-derived xenografts of gastric cancer and lung cancer, respectively. In particular, DM004 Top2-MMAE outperformed benchmark ADCs in lung BP0508 PDX models. In summary, we have identified a novel BsADC which may be a promising future treatment for cancers co-expressing 5T4 and MET.

## 5T4 and MET are expressed in multiple tumor types

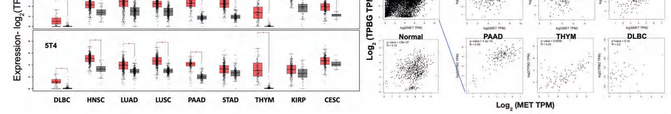


(A) Expression of 5T4 and MET in different cancer types (GEPIA2[1]).
5T4 (also known as TPBG) and MET are highly expressed in a variety of cancer types, including lung adenocarcinoma (LUAD), lung squamous cell carcinoma (LUSC) and head and neck squamous cell carcinoma (HNSC) . PAAD, Pancreatic Ductal Adenocarcinoma. STAD, stomach adenocarcinoma. THYM, Thymoma. KIRP, kidney renal papillary cell carcinoma. CESC, cervical cancer.

References:
1 Tang Z., Kang B., Li C., Chen T., Zhang Z. (2019) GEPIA2: an enhanced web server for large-scale expression profiling and interactive analysis. Nucleic Acids Res, 47(W1):W556-W560. doi: 10.1093/nar/gkz430.

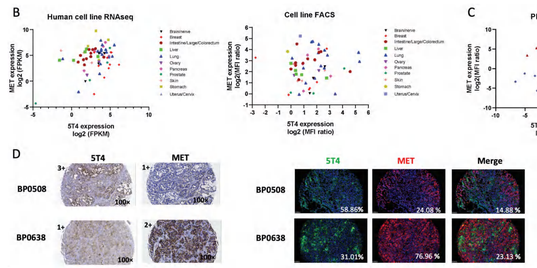


(B-C) Expression of 5T4 and MET in cell lines and patient-derived xenografts (PDX) measured by RNA-seq or FACS as indicated. FACS and RNA-seq data in (C) represent different cell lines.
Co-expression of 5T4 and MET detected in a variety of human tumor cell lines and Patient derived xenografts (PDX) by RNAseq.
(D) Representative images of 5T4/MET immunohistochemistry/immunofluorescence staining (percentages indicate numbers of positive cells/total cells, using Halo® Image Analysis Platform) indicate intra-tumor heterogeneity of expression. Both BP0508 and BP0638 are human lung cancer samples.

## Annotation of test articles

| Antibodies | Annotation |
|---|---|
| anti-5T4 | 5T4 binder |
| anti-MET1 | MET binder 1 |
| anti-MET2 | MET binder 2 |
| anti-5T4 monovalent | parental monovalent anti-5T4 |
| anti-MET1 monovalent | parental monovalent anti-MET1 |
| anti-MET2 monovalent | parental monovalent anti-MET2 |
| Top1 | BsAbs, anti-5T4 x anti-MET1 |
| Top2 | BsAbs, anti-5T4 x anti-MET2 |
| PF-06263507-analog | 5T4 benchmark |
| Telisotuzumab-analog | MET benchmark |
| Isotype | negative control |

## Identification of an anti-5T4 antibody with strong avidity and specificity

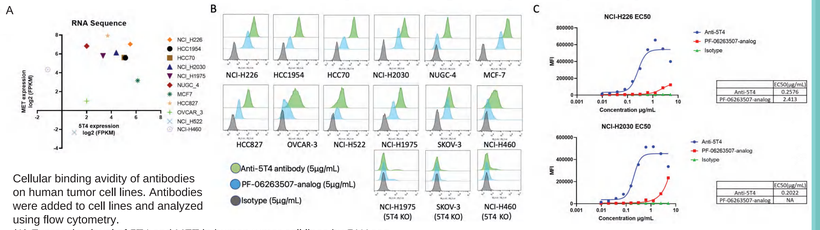


Cellular binding avidity of antibodies on human tumor cell lines. Antibodies were added to cell lines and analyzed using flow cytometry.
(A) Expression level of 5T4 and MET in human tumor cell lines by RNAseq.
(B,C) anti-5T4 binder shows outstanding binding avidity and specificity in a variety of human tumor cell lines compared to PF-06263507-analog.
Anti-5T4 binder demonstrated excellent avidity for a variety of tumor cell lines, suggesting that the DM004 has potential for expanded patient response rates in clinical study.

## Binding capacity of DM004 (5T4 x MET) BsAbs

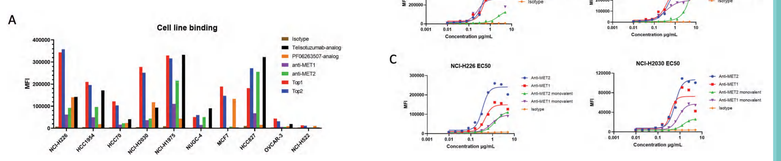


Cellular binding kinetics of antibodies on human tumor cell lines. Antibodies were added to cell lines and analyzed using flow cytometry.
(A,B) DM004 BsAb candidates (Top1 and Top2) had high binding avidity in multiple human tumor cell lines with different expression levels of 5T4 and MET (shown in panel 4A). (C) Anti-MET1 and anti-MET2 demonstrated higher binding avidity in NCI-H226 and NCI-H2030 than their respective monovalent antibodies, suggesting that the anti-MET binding of DM004 may have better tumor selectivity, which may help to overcome the on-target toxicity of MET-ADC already observed in clinical study.

## Internalization of DM004 BsAbs

Internalization of DM004 BsAbs. Antibodies plus the pHAb-AffiniPure Fab Goat Anti-Human IgG secondary antibody were added to NCI-H226 or NCI-H2030 cell lines, respectively, and incubated 0, 3 and 6 hours. Data was collected by flow cytometry. (A) The monovalent anti-5T4, anti-MET1 and anti-MET2 displayed decreased endocytosis when compared to parental monoclonal antibody, respectively. (B) Compared to benchmarks, DM004 BsAbs candidates showed more robust endocytosis than PF-06263507-analog and Telisotuzumab-analog, and enhanced internalization compared to its parental monoclonal and monovalent anti-5T4 and anti-MET antibodies.

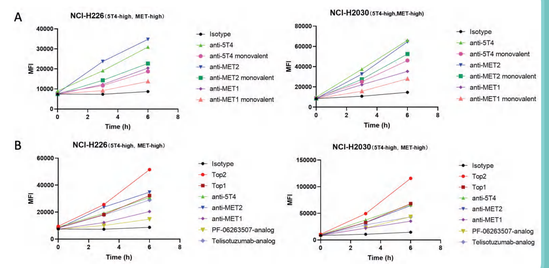


## *In vitro* cytotoxicity of DM004 candidates

In vitro cytotoxicity of DM004. ADCs (DAR~4) were added to NCI-H226 cell lines, and killing activity was detected after 72h of incubation with IncuCyte (Sartorius AG, IncuCyte® S3). Phase object confluence was analyzed. (A) DM004 candidates showed potent cytotoxicity activity. (B) Anti-5T4-MMAE showed strong cytotoxicity activity when compared to 5T4 benchmark ADC, suggesting that the 5T4 arm of DM004 has stronger tumor killing ability.

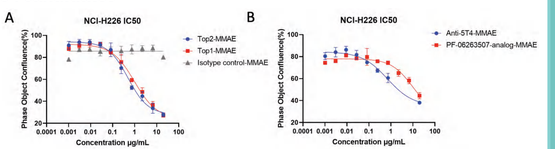


| | IC50(μg/mL) |
|---|---|
| TOP1-MMAE | 0.9855 |
| TOP2-MMAE | 0.5044 |

| | IC50(μg/mL) |
|---|---|
| Anti-5T4-MMAE | 0.6996 |
| PF-06263507-analog-MMAE | 9.533 |

## Anti-5T4-MMAE *in vivo* efficacy in PDX models

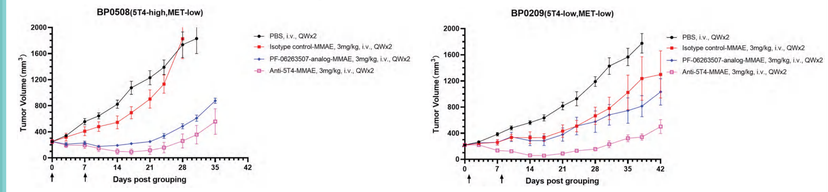


In vivo efficacy studies in PDX models with different expression levels of 5T4 (BP0508, lung cancer; BP0209, pancreatic cancer). Patient-derived tumor fragments (2x2x2 mm) were subcutaneously engrafted into the right flank of female B-NDG (immunodeficient) mice. When tumor volume reached approximately 200 mm³, the mice were randomly placed into different groups (n=5/group) based on tumor volumes. The mice were then intravenously injected (i.v.) with PBS or ADCs (DAR~4). Administrations are indicated by arrows.

- **In both PDX models, anti-5T4-MMAE displayed more effective anti-tumor activity than PF-06263507-analog-MMAE.**

## *In vivo* efficacy of DM004 candidates in CDX models

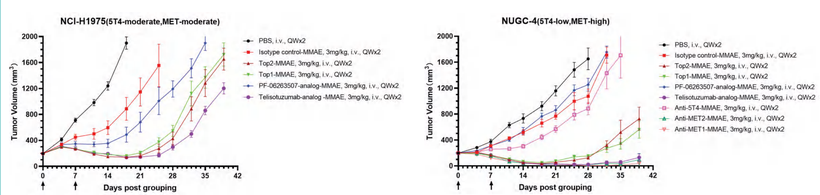


In vivo efficacy studies in CDX models. Tumor cells were implanted subcutaneously into the right flank of female B-NDG (immunodeficient) mice. When tumor volume reached approximately 200 mm³, the mice were randomly placed into different groups (n=5/group) based on tumor volumes. The mice were then intravenously injected (i.v.) with PBS or ADCs (DAR~4). Administration timepoints are indicated by arrows.

- **In both NCI-H1975 and NUGC-4 models, DM004 BsADC candidates exhibited better anti-tumor activity than PF-06263507-analog-MMAE.**

## *In vivo* efficacy of DM004 candidates in PDX models

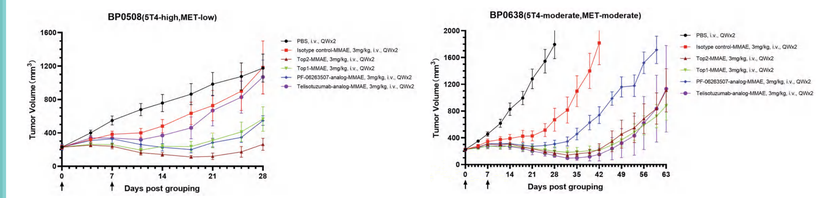


In vivo efficacy studies of DM004 in lung cancer PDX models. Patient-derived tumor fragments (2x2x2 mm) were subcutaneously engrafted into the right flank of female B-NDG (immunodeficient) mice. When tumor volume reached approximately 200 mm³, the mice were randomly placed into different groups (n=5/group) based on tumor volume. The mice were then intravenously injected (i.v.) with PBS or ADCs (DAR~4). Timepoints of administration are indicated by arrows.

- **DM004 BsADC candidates demonstrated robust anti-tumor activity in both PDX models. In particular, Top2-MMAE outperformed benchmark ADCs in the BP0508 model.**

## SUMMARY

- DM004's parental 5T4 ADC shows excellent anti-tumor efficacy both *in vitro* and *in vivo*.
- The reduced binding avidity of anti-MET monovalent antibodies suggests improved tumor selectivity for DM004 compared to anti-MET monoclonal antibody.
- DM004 BsADC candidates demonstrate robust anti-tumor efficacy in CDX and PDX models with different levels of 5T4 and MET expression, indicating DM004 has a strong potential for clinical benefit.